

Supporting Information: Scalable dynamic characterization of synthetic gene circuits

Neil Dalchau, Paul K. Grant, Prashant Vaidyanathan, Colin Gravill, Carlo Spaccasassi, and Andrew Phillips

Biological Computation group, Microsoft Research, Cambridge, CB1 2FB, UK

Contents

S1 Model implementation using the GEC & CRN language	2
S1.1 Extensions to CRN	2
S1.2 Extensions to GEC	2
S1.3 Dynamic Characterization - Wrapper Program	4
S2 Models of cells expressing synthetic gene circuits	14
S2.1 No plasmid (Autofluorescence)	14
S2.2 Constitutive expression via the PR promoter	18
S2.3 HSL Double Receivers	23
S2.4 AHL senders (Relays)	34
S2.5 Inducible expression (PBAD)	40
S2.6 HSL lactonase (AiiA)	43
S3 Supplementary Figures and Tables	51

S1 Model implementation using the GEC & CRN language

To carry out dynamic characterization, we have extended the chemical reaction network (CRN) and genetic engineering of cells (GEC) languages and associated toolchain. In this section, the extensions made to CRN and GEC is discussed. This section also highlights a wrapper program that eases the the preparation and scheduling of inference tasks across a graph (Fig. 3), including the collection of multiple MCMC chains and using these to marginalize and approximate distributions as Gaussian priors.

S1.1 Extensions to CRN

The main extension to CRN is the ability to define an Inference Graph. Inference Graphs provide a graphical method to chain inference problems. An Inference Graph consists of:

nodes which denote inference problems. Each node consists of a set of CRN systems [1] as well as inference settings.

edges which represent the propagation of parameter distributions or values from one inference problem to another. Each edge is directed and consists of a *from* node, a *to* node as well a list of parameters to be propagated along with the associated propagation property. The *from* node indicates the node (or a specific CRN system within a node) from which the posteriors of inferred parameters are propagated. The *to* node indicates the downstream Node (or CRN system within the node) for which the inferred parameters in *from* node as used as priors. Each parameter in an edge as a property (*Normal* or *Fixed* which indicated whether the full parameter distribution or the parameter value will be propagated.

The syntax of inference graphs is defined as follows, where italicized names denote syntax variables:

```
Property ::=
| Fixed
| Normal
| TruncatedNormal
```

```
Parameter ::=
— Name
— Name = Property
```

```
Parameters ::= [Parameter1; ...; ParameterN]
```

```
Edge ::=
| edge Name — > Parameters Name
| edge Name.Name — > Parameters Name.Name
```

```
Node ::=
node Name {
  systems = [Name1; ...; NameN];
  settings = Inference_settings;
}
```

We use a dot notation to refer to a specific device at a given node in the graph. Note that we also allow edges between nodes directly, to indicate that the parameters are shared between all devices present at the node.

When a CRN program has an inference graph, it is structured into the following sections: *directives*, *modules*, *systems*, and *inference graph*.

S1.2 Extensions to GEC

To enable the generation of models for dynamic characterization, we have extended the GEC language [2] which was developed to express interactions between DNA and chemical components in a modular manner.

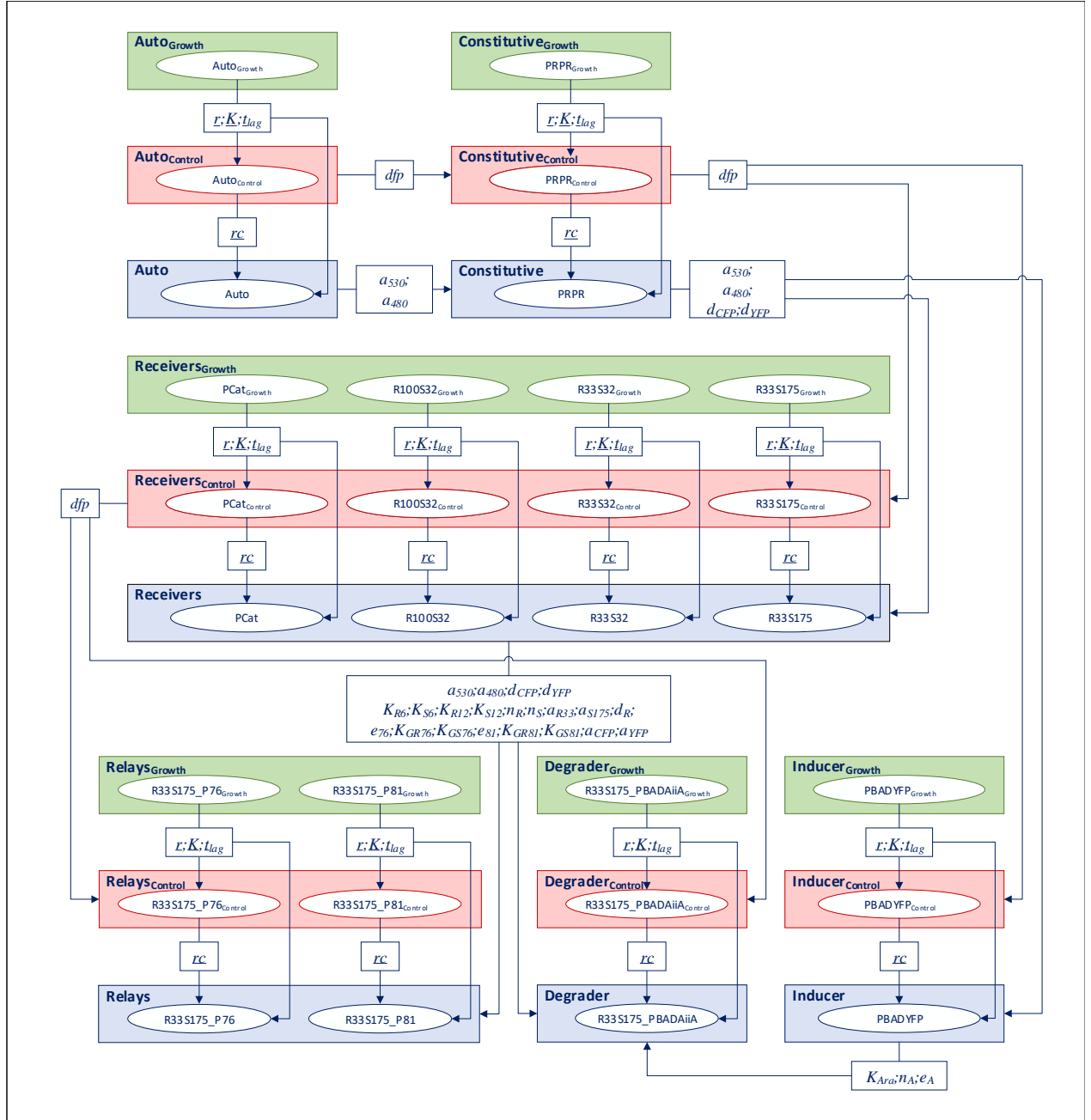


Figure S1: Inference graph for ratiometric dynamic characterization of the case study presented in the main text.

The two main extensions can be summarized as follows:

- Ability to specify devices - GEC previously only supported promoters, rbs, pcr (protein coding regions - also known as cds or coding sequences), and terminators as the basic part types. We have now extended the language to allow users to specify a device. A device consists of basic parts types (promoters, rbs, pcr, and terminators) and other devices and can be used to link the model of a biochemical process to the structural topology responsible for the process.
- Introduction of crn modules, systems, and inference graphs - The syntax of GEC has been modified to closely resemble the structure of a CRN program [1]. We have extended GEC to include CRN directives, CRN modules, systems, and inference graphs to enable the generation of inference graphs using which dynamic characterization can be carried out.

A GEC program can be divided into the following sections:

directives are settings that describe how a GEC program must be executed. Directives are specified using the `directive` keyword. We have modified GEC to use CRN directives and have introduced three directives that are specific to GEC:

- `RMRNADeg` - allows users to specify the rate of mRNA degradation (the default value is 0.001)
- `crn` - allows users to specify CRN instructions (module invocation, initials, and reactions) which is concatenated with the crn instructions generated for a GEC program.
- `override` - allows users to specify CRN instructions that replace the crn instructions generated for a GEC program.

module definitions are subroutines (or procedures) used in the crn language. Modules are defined using the `module` keyword, and consist of crn instructions and other module definitions. A module definition can have zero or more arguments.

device model definitions are module definitions that describe the model of a device. Device model definitions are defined using the `device` keyword, followed by the device name, with zero or more arguments and consist of crn instructions and other module definitions and module invocations. The structural definition (part and device components) of the device is specified in the GEC Parts and Device library.

templates are subroutines (or procedures) for the GEC language. Templates are defined using the `template` keyword and contain part types, part variables, part properties, normal reactions, and transport reactions. Like modules, templates can have zero or more arguments.

systems are modular units of a GEC program that describe a specific cell line, genetic circuit, or biochemical process. Systems are structurally and functionally distinct from one another. A system can have directives, modules, module invocations, template invocations, parts and their properties, and GEC reactions (normal and transport reactions) whose scope is local to that system. A GEC program can also have the aforementioned program components outside a system. These components are considered to be *top level* and their scope is global to the entire GEC program. A system is defined using the keyword `system`.

inference graph is a graph that consists of nodes and edges that describe the inference tasks that span across a graph. The graph is described using the `node` and `edge` keywords.

S1.3 Dynamic Characterization - Wrapper Program

All models are written in GEC or CRN, which have a default file format for observational data. A wrapper program simplifies the use of data and the specification of *sweeps* (which can be used to specify treatment concentrations or input signals) by automatically extracting these from a more structured data file (see Supplementary Data for examples). To specify how the observational data is to be loaded for each model and each inference node, a YAML configuration file must be loaded. An example YAML file is shown as:

```

1 homedir: ..\..\..\
2 outdir: GEC
3 hypothesis: Constant_Ratiometric
4 cellmodel: laglogistic
5 preprocess: individual
6 files: [proc_EC10G_EtOH]
7 inputs: [EtOH]
8 nodes:
9 - { node: Auto_Growth, signal: OD, targets: [ {device: EC10G, model: growth} ] }
10 - { node: Auto_Control, signal: RFP, targets: [ {device: EC10G, model: control} ] }
11 - { node: Auto, signal: YFP_CFP, targets: [ {device: EC10G, model: auto} ] }

```

In the wrapper program, devices and associated measurements are specified for inclusion, and a name is given to an inference problem. A YAML file must be provided that specifies how to load the data files appropriately, including the name(s) of the measurement signal(s) used in a given inference node, and the names of the devices associated with each model in that inference node. As an example, one can specify the characterization of the growth phase of the Auto circuit by calling:

```
DynamicCharacterization.exe graph --node Auto_Growth --yaml Ratiometric --hypothesis TargetSwitch --seed 0
```

The code in Listing 1 shows the complete GEC code used to evaluate the Constant hypothesis.

In the following section (S2), the model of each circuit is explained in detail.

Listing 1: Complete code for Constant hypothesis

```

1 directive simulator sundials
2 directive plot_settings { x_label = "Time (h)"; y_label = "Fluorescence (a.u.)" }
3 directive parameters [
4   // Treatments
5   C6=0.0; C12=0.0; Ara=0.0; tau=0.0;
6   // Cell growth
7   c0 = 0.002;
8   // Autofluorescence
9   a530=1e0, { distribution=Uniform(1e-3,1e3) };
10  a480=1e0, { distribution=Uniform(1e-3,1e3) };
11  // FP
12  dRFP=0.1, { distribution=Uniform(1e-3,1e0) };
13  dCFP=1e-2, { distribution=Uniform(1e-3,1e0) };
14  dYFP=1e-2, { distribution=Uniform(1e-3,1e0) };
15  // Double receiver
16  KR6=1e-2, { distribution=Uniform(1e-8,1e0) };
17  KS6=1e-4, { distribution=Uniform(1e-8,1e0) };
18  KR12=1e-3, { distribution=Uniform(1e-8,1e0) };
19  KS12=1e-2, { distribution=Uniform(1e-8,1e0) };
20  nR=0.797, { interval=Real; distribution=Uniform(0.5,2.0) };
21  nS=0.797, { interval=Real; distribution=Uniform(0.5,2.0) };
22  aR100=1.0, { distribution=Uniform(1e0,1e2) };
23  aR33=1.0, { distribution=Uniform(1e0,1e2) };
24  aS32=1.0, { distribution=Uniform(1e0,1e2) };
25  aS175=1.0, { distribution=Uniform(1e0,1e2) };
26  dR=0.1, { distribution=Uniform(1e-2,1e1) };
27  //dS=0.1, { distribution=Uniform(1e-2,1e2) };
28  e76=1e-2, { distribution=Uniform(1e-4,1.0) };
29  KGR_76=1e-2,{ distribution=Uniform(1e-4,1e0) };
30  KGS_76=1e-6,{ distribution=Uniform(1e-8,1e0) };
31  e81=1e-2, { distribution=Uniform(1e-4,1.0) };
32  KGR_81=1e-6,{ distribution=Uniform(1e-8,1e0) };
33  KGS_81=1e-2,{ distribution=Uniform(1e-4,1e0) };
34  aCFP=1e3, { distribution=Uniform(1e0,1e5) };
35  aYFP=1e3, { distribution=Uniform(1e0,1e5) };

```

```

36 dCFP=1e-2, { distribution=Uniform(1e-3,1e0) };
37 dYFP=1e-2, { distribution=Uniform(1e-3,1e0) };
38 // Relay P81-LuxI
39 kC6=1e0, { distribution=Uniform(1e0,1e6) };
40 Klux=1.0, { distribution=Uniform(1e0,1e6) };
41 dluxI=0.1,{ distribution=Uniform(1e-3,1e1) };
42 // Relay P76-LasI
43 kC12=1e0, { distribution=Uniform(1e0,1e6) };
44 Klas=1.0, { distribution=Uniform(1e0,1e6) };
45 dlasI=0.1,{ distribution=Uniform(1e-3,1e1) };
46 // PBad
47 KAra=1.0, { distribution=Uniform(1e-2,1e2) };
48 nA=1.0, { interval=Real; distribution=Uniform(0.5,3.0) };
49 eA=0.1, { interval=Real; distribution=Uniform(0.0,0.5) };
50 // AiiA
51 dA6=1e-1, { distribution=Uniform(1e-3,1e1) };
52 dA12=1e-1, { distribution=Uniform(1e-3,1e1) };
53 daiiA=0.1, { distribution=Uniform(1e-3,1e1) };
54 ]
55 directive inference { burnin=200; samples=200; thin=20; noise_model = proportional }
56 directive simulation {multicore=True}
57 directive rates [
58   growth = [grow]*r*(1 - [x] / K);
59   capacity = rc;
60   boundLuxR = [luxR]^2 * ((KR6*[c6])^nR + (KR12*[c12])^nR) / ((1.0 + KR6*[c6] + KR12*[c12])^nR);
61   boundLasR = [lasR]^2 * ((KS6*[c6])^nS + (KS12*[c12])^nS) / ((1.0 + KS6*[c6] + KS12*[c12])^nS);
62   P76 = (e76 + KGR_76*[boundLuxR] + KGS_76*[boundLasR]) / (1.0 + KGR_76*[boundLuxR] +
63     KGS_76*[boundLasR]);
64   P81 = (e81 + KGR_81*[boundLuxR] + KGS_81*[boundLasR]) / (1.0 + KGR_81*[boundLuxR] +
65     KGS_81*[boundLasR]);
66   PBad = (Ara^nA+eA*KAra^nA)/(Ara^nA+KAra^nA);
67   one = 1.0;
68 ]
69 directive sweeps [
70   sweep_R33S175_PBADAiiA = [(C6,C12,Ara) = [(25000,0,5); (25000,0,2.5); (25000,0,1.25);
71     (25000,0,0.625); (25000,0,0.3125); (25000,0,0); (0,25000,5); (0,25000,2.5); (0,25000,1.25);
72     (0,25000,0.625); (0,25000,0.3125); (0,25000,0); (5000,0,5); (5000,0,2.5); (5000,0,1.25);
73     (5000,0,0.625); (5000,0,0.3125); (5000,0,0); (0,5000,5); (0,5000,2.5); (0,5000,1.25);
74     (0,5000,0.625); (0,5000,0.3125); (0,5000,0); (1000,0,5); (1000,0,2.5); (1000,0,1.25);
75     (1000,0,0.625); (1000,0,0.3125); (1000,0,0); (0,1000,5); (0,1000,2.5); (0,1000,1.25);
76     (0,1000,0.625); (0,1000,0.3125); (0,1000,0); (200,0,5); (200,0,2.5); (200,0,1.25);
77     (200,0,0.625); (200,0,0.3125); (200,0,0); (0,200,5); (0,200,2.5); (0,200,1.25);
78     (0,200,0.625); (0,200,0.3125); (0,200,0); (40,0,5); (40,0,2.5); (40,0,1.25); (40,0,0.625);
79     (40,0,0.3125); (40,0,0); (0,40,5); (0,40,2.5); (0,40,1.25); (0,40,0.625); (0,40,0.3125);
80     (0,40,0); (8,0,5); (8,0,2.5); (8,0,1.25); (8,0,0.625); (8,0,0.3125); (8,0,0); (0,8,5);
81     (0,8,2.5); (0,8,1.25); (0,8,0.625); (0,8,0.3125); (0,8,0); (1.6,0,5); (1.6,0,2.5);
82     (1.6,0,1.25); (1.6,0,0.625); (1.6,0,0.3125); (1.6,0,0); (0,1.6,5); (0,1.6,2.5);
83     (0,1.6,1.25); (0,1.6,0.625); (0,1.6,0.3125); (0,1.6,0); (0,0,5); (0,0,2.5); (0,0,1.25);
84     (0,0,0.625); (0,0,0.3125); (0,0,0); (0,0,5); (0,0,2.5); (0,0,1.25); (0,0,0.625);
85     (0,0,0.3125); (0,0,0)]];
86   sweep_C6C12_double = [(C6,C12) = [(25000,0); (8333.3333333333,0); (2777.7777777778,0);
87     (925.925925925926,0); (308.641975308642,0); (102.880658436214,0); (34.2935528120713,0);
88     (11.4311842706904,0); (3.81039475689681,0); (1.27013158563227,0); (0.423377195210757,0);
89     (0,0); (0,25000); (0,8333.3333333333); (0,2777.7777777778); (0,925.925925925926);
90     (0,308.641975308642); (0,102.880658436214); (0,34.2935528120713); (0,11.4311842706904);
91     (0,3.81039475689681); (0,1.27013158563227); (0,0.423377195210757); (0,0);(25000,0);
92     (8333.3333333333,0); (2777.7777777778,0); (925.925925925926,0); (308.641975308642,0);
93     (102.880658436214,0); (34.2935528120713,0); (11.4311842706904,0); (3.81039475689681,0);

```

```

(1.27013158563227,0); (0.423377195210757,0); (0,0); (0,25000); (0,8333.333333333333);
(0,2777.777777777778); (0,925.925925925926); (0,308.641975308642); (0,102.880658436214);
(0,34.2935528120713); (0,11.4311842706904); (0,3.81039475689681); (0,1.27013158563227);
(0,0.423377195210757); (0,0)]];
71 sweep_C6C12 = [(C6,C12) = [(25000,0); (8333.33333333333,0); (2777.77777777778,0);
(925.925925925926,0); (308.641975308642,0); (102.880658436214,0); (34.2935528120713,0);
(11.4311842706904,0); (3.81039475689681,0); (1.27013158563227,0); (0.423377195210757,0);
(0,0); (0,25000); (0,8333.33333333333); (0,2777.77777777778); (0,925.925925925926);
(0,308.641975308642); (0,102.880658436214); (0,34.2935528120713); (0,11.4311842706904);
(0,3.81039475689681); (0,1.27013158563227); (0,0.423377195210757); (0,0)]];
72 sweep_relays = [(C6,C12) = [(25000,0); (8333.333333,0); (2777.777778,0); (925.925926,0);
(308.641975,0); (102.880658,0); (34.293553,0); (11.431184,0); (3.810395,0); (1.270132,0);
(0.423377,0); (0,0); (0,25000); (0,8333.333333); (0,2777.777778); (0,925.925926);
(0,308.641975); (0,102.880658); (0,34.293553); (0,11.431184); (0,3.810395); (0,1.270132);
(0,0.423377); (0,0); (25000,0); (8333.333333,0); (2777.777778,0); (925.925926,0);
(308.641975,0); (102.880658,0); (34.293553,0); (11.431184,0); (3.810395,0); (1.270132,0);
(0.423377,0); (0,0); (0,25000); (0,8333.333333); (0,2777.777778); (0,925.925926);
(0,308.641975); (0,102.880658); (0,34.293553); (0,11.431184); (0,3.810395); (0,1.270132);
(0,0.423377); (0,0)]];
73 sweep_PBAD_eYFP = [(Ara) = [(25); (0.78); (12.5); (0.39); (6.25); (0.195); (3.125); (0.0975);
(1.5625); (0.04875); (0.78125); (0.024375)]];
74 ]
75
76 module CFP(P,a,growth,capacity) = {
77   ->[[capacity]*a*[P]] cfp |
78   cfp ->{dCFP} |
79   cfp ->[[growth]*[cfp]]
80 }
81 module YFP(P,a,growth,capacity) = {
82   ->[[capacity]*a*[P]] yfp |
83   yfp ->{dYFP} |
84   yfp ->[[growth]*[yfp]]
85 }
86 module LuxR(aR,growth,capacity) = {
87   ->[[capacity]*aR] luxR |
88   luxR ->{dR} |
89   luxR ->[[growth]*[luxR]]
90 }
91 module LasR(aS,growth,capacity) = {
92   ->[[capacity]*aS] lasR |
93   lasR ->{dR} |
94   lasR ->[[growth]*[lasR]]
95 }
96 module LuxI(P,growth,capacity) = {
97   ->[[capacity]*[P]] luxI |
98   luxI ->{dluxI} |
99   luxI ->[[growth]*[luxI]] |
100  ->[kC6*[capacity]*[x]*[luxI]/(1+[luxI]/Klux)] c6
101 }
102 module LasI(P,growth,capacity) = {
103   ->[[capacity]*[P]] lasI |
104   lasI ->{dlasI} |
105   lasI ->[[growth]*[lasI]] |
106   ->[kC12*[capacity]*[x]*[lasI]/(1+[lasI]/Klas)] c12
107 }
108 module AiiA(P,aI,growth,capacity) = {
109   ->[[capacity]*aI*[P]] aiiA |
110   aiiA ->{daiiA} |
111   aiiA ->[[growth]*[aiiA]] |

```

```

112     c6 -> [[x]*dA6*[c6]*[aiiA]] |
113     c12 -> [[x]*dA12*[c12]*[aiiA]]
114 }
115 module cells(growth,tlag) = {
116     init x c0 | init grow 1 @ tlag |
117     init c6 C6 @ tau | init c12 C12 @ tau |
118     ->[[growth]*[x]] x
119 }
120 module autofluorescence(growth,capacity) = {
121     ->[[capacity]*a530] f530 |
122     f530 ->[[growth]*[f530]] |
123     ->[[capacity]*a480] f480 |
124     f480 ->[[growth]*[f480]]
125 }
126 module doublereceiver(aR,aS,growth,capacity) = {
127     LuxR(aR,growth,capacity) |
128     LasR(aS,growth,capacity) |
129     YFP(P81,aYFP,growth,capacity) |
130     CFP(P76,aCFP,growth,capacity)
131 }
132
133 // Models of each GEC device
134 device prpr() = { YFP(one,aYFP,growth,capacity) | CFP(one,aCFP,growth,capacity) }
135 device drPCat() = { doublereceiver(1.0,1.0,growth,capacity) }
136 device drR100S32() = { doublereceiver(aR100,aS32,growth,capacity) }
137 device drR33S32() = { doublereceiver(aR33,aS32,growth,capacity) }
138 device drR33S175() = { doublereceiver(aR33,aS175,growth,capacity) }
139 device relayP76LasI() = { LasI(P76,growth,capacity) }
140 device relayP81LuxI() = { LuxI(P81,growth,capacity) }
141 device pBADYFP() = { YFP(PBad,aYFP,growth,capacity) }
142 device pBADAiiA() = { AiiA(PBad,1.0,growth,capacity) }
143
144 // Systems for growth and control that will be reused heavily
145 system growth = {
146     directive simulation { final=36.0; points=250; plots=[[x]+x0]; multicore=True}
147     directive plot_settings { y_label = "OD" }
148     directive parameters [
149         r = 1, { interval=Real; distribution=Uniform(0.1,10); variation=Multiple };
150         K = 2, { interval=Real; distribution=Uniform(0.1,5); variation=Multiple };
151         tlag = 1, { interval=Real; distribution=Uniform(0,10); variation=Multiple };
152         x0=0.1,{ interval=Real; distribution=Uniform(0.0,0.2) };
153     ]
154     directive rates [growth = [grow]*r*(1 - [x] / K)]
155     directive crn { cells(growth,tlag) }
156 }
157 system control = {
158     directive simulation { final=36.0; points=250; plots=[[x]*[fp]+f0]; plotcolours=["#FF0000"];
159         multicore=True}
160     directive plot_settings { y_label = "RFP fluorescence (a.u.)" }
161     directive parameters [
162         r = 1, { interval=Real; distribution=Uniform(0.1,10); variation=Multiple };
163         K = 2, { interval=Real; distribution=Uniform(0.1,5); variation=Multiple };
164         tlag = 1, { interval=Real; distribution=Uniform(0,10); variation=Multiple };
165         rc=1e2, { distribution=Uniform(1e0,1e5); variation=Multiple };
166         f0=100.0,{ interval=Real; distribution=Uniform(0.0,10000.0) };
167     ]
168     directive rates [growth = [grow]*r*(1 - [x] / K);capacity = rc]
169     directive crn {
170         cells(growth,tlag)

```



```

170     | fp ->[[growth]*[fp]]    // Dilution
171     | ->[[capacity]] fp      // Transcription/translation
172     | fp ->{dRFP}           // Degradation
173 }
174 }
175 system target = {
176     directive simulation { final=36.0; points=250; plots=[[x]*([yfp]+[f530])+b530;
177         [x]*([cfp]+[f480])+b480]; plotcolours=["#FFDF00"; "#ADD8E6" ] }
178     directive parameters [
179         r = 1, { interval=Real; distribution=Uniform(0.1,10); variation=Multiple };
180         K = 2, { interval=Real; distribution=Uniform(0.1,5); variation=Multiple };
181         tlag = 1, { interval=Real; distribution=Uniform(0,10); variation=Multiple };
182         rc=1e2, { distribution=Uniform(1e0,1e5); variation=Multiple };
183         b530=1e3, { interval=Real; distribution=Uniform(0.0,5e3) };
184         b480=1e3, { interval=Real; distribution=Uniform(0.0,1e4) };
185     ]
186     directive rates [growth = [grow]*r*(1 - [x] / K);capacity = rc]
187     directive crn { cells(growth,tlag) | autofluorescence(growth,capacity) }
188 }
189
190 //Autofluorescence
191 system auto_growth = { growth with
192     directive simulation {sweeps=[sweep_R33S175_PBADAiiA] }
193     directive data [EC10G_OD]
194 }
195
196 system auto_control = { control with
197     directive simulation { final=36.0; points=250; plots=[[x]*[fp]+f0]; plotcolours=["#FF0000"];
198         multicore=True; sweeps=[sweep_R33S175_PBADAiiA] }
199     directive data [EC10G_mRFP1]
200 }
201
202 system auto = { target with
203     directive simulation { final=36.0; points=250; plots=[[x]*[f530]+b530; [x]*[f480]+b480];
204         plotcolours=["#FFDF00"; "#ADD8E6"]; multicore=True; sweeps=[sweep_EC10G_dataset0] }
205     directive sweeps [
206         sweep_EC10G_dataset0 = [(EtOH, chlor, C6, C12, Ara) = [(1700000000,0,0,0,0);
207             (170000000,0,0,0,0); (17000000,0,0,0,0); (170000,0,0,0,0);
208             (17000,0,0,0,0); (1700,0,0,0,0); (170,0,0,0,0); (17,0,0,0,0); (1.7,0,0,0,0);
209             (0.17,0,0,0,0); (0,0,0,0,0); (1700000000,0,0,0,0); (170000000,0,0,0,0);
210             (17000000,0,0,0,0); (170000,0,0,0,0); (17000,0,0,0,0); (1700,0,0,0,0);
211             (170,0,0,0,0); (17,0,0,0,0); (1.7,0,0,0,0); (0.17,0,0,0,0);
212             (0,0,0,0,0); (1700000000,0,0,0,0); (170000000,0,0,0,0); (17000000,0,0,0,0);
213             (170000,0,0,0,0); (17000,0,0,0,0); (1700,0,0,0,0); (170,0,0,0,0); (17,0,0,0,0);
214             (1.7,0,0,0,0); (0.17,0,0,0,0); (0,0,0,0,0); (1700000000,0,0,0,0);
215             (170000000,0,0,0,0); (17000000,0,0,0,0); (170000,0,0,0,0); (17000,0,0,0,0);
216             (1700,0,0,0,0); (170,0,0,0,0); (17,0,0,0,0); (1.7,0,0,0,0);
217             (0.17,0,0,0,0); (0,0,0,0,0)]];
218     ]
219     directive data [EC10G_EYFP_ECFP]
220 }
221
222 //Constitutive
223 system prpr_growth = { growth with
224     directive simulation {sweeps=[sweep_R33S175_PBADAiiA] }
225     directive data [PRPR_OD]
226 }
227
228

```

```

215 system prpr_control = { control with
216     directive simulation { final=36.0; points=250; plots=[[x]*[fp]+f0]; plotcolours=["#FF0000"];
        multicore=True; sweeps=[sweep_R33S175_PBADaiiA] }
217     directive data [PRPR_mRFP1]
218 }
219
220 system prpr = { target with
221     directive simulation {multicore=True; sweeps=[sweep_PLPL_dataset1]}
222     directive parameters [
223         r = 1, { interval=Real; distribution=Uniform(0.1,10); variation=Multiple };
224         K = 2, { interval=Real; distribution=Uniform(0.1,5); variation=Multiple };
225         tlag = 1, { interval=Real; distribution=Uniform(0,10); variation=Multiple };
226         rc=1e2, { distribution=Uniform(1e0,1e5); variation=Multiple };
227         aCFP=1e3, { distribution=Uniform(1e0,1e5); variation=Random };
228         aYFP=1e3, { distribution=Uniform(1e0,1e5); variation=Random };
229         b530=1e3, { interval=Real; distribution=Uniform(0.0,5e3) };
230         b480=1e3, { interval=Real; distribution=Uniform(0.0,1e4) };
231     ]
232     directive sweeps [
233         sweep_PLPL_dataset1 = [(EtOH, chlor, C6, C12, Ara) = [(0,5,0,0,0); (0,5,0,0,0); (0,2.5,0,0,0);
                (0,2.5,0,0,0); (0,1.25,0,0,0); (0,1.25,0,0,0); (0,0.625,0,0,0); (0,0.625,0,0,0);
                (0,0.3125,0,0,0); (0,0.3125,0,0,0); (0,0,0,0,0); (0,0,0,0,0)]];
234     ]
235     directive data [PRPR_EYFP_ECFP]
236     prpr:device
237 }
238
239 // DR (PCat-PCat)
240 system PCat_growth = { growth with
241     directive simulation {multicore=True; sweeps=[sweep_C6C12_double]}
242     directive data [PCat_OD]
243 }
244
245 system PCat_control = { control with
246     directive simulation {multicore=True; sweeps=[sweep_C6C12_double]}
247     directive data [PCat_mRFP1]
248 }
249
250 system PCat = { target with
251     directive simulation {multicore=True; sweeps=[sweep_C6C12_double]}
252     directive data [PCat_EYFP_ECFP]
253     drPCat:device
254 }
255
256 // DR (R100-S32)
257 system R100S32_growth = { growth with
258     directive simulation {multicore=True; sweeps=[sweep_C6C12]}
259     directive data [R100S32_OD]
260 }
261
262 system R100S32_control = { control with
263     directive simulation {multicore=True; sweeps=[sweep_C6C12]}
264     directive data [R100S32_mRFP1]
265 }
266
267 system R100S32 = { target with
268     directive simulation {multicore=True; sweeps=[sweep_C6C12]}
269     directive data [R100S32_EYFP_ECFP]
270     drR100S32:device

```

```

271 }
272
273 // DR (R33-S32)
274 system R33S32_growth = { growth with
275     directive simulation {multicore=True; sweeps=[sweep_C6C12]}
276     directive data [R33S32_OD]
277 }
278
279 system R33S32_control = { control with
280     directive simulation {multicore=True; sweeps=[sweep_C6C12]}
281     directive data [R33S32_mRFP1]
282 }
283 system R33S32 = { target with
284     directive simulation {multicore=True; sweeps=[sweep_C6C12]}
285     directive data [R33S32_EYFP_ECFP]
286     drR33S32:device
287 }
288
289 // DR (R33-S175)
290 system R33S175_growth = { growth with
291     directive simulation {multicore=True; sweeps=[sweep_C6C12]}
292     directive data [R33S175_OD]
293 }
294
295 system R33S175_control = { control with
296     directive simulation {multicore=True; sweeps=[sweep_C6C12]}
297     directive data [R33S175_mRFP1]
298 }
299 system R33S175 = { target with
300     directive simulation {multicore=True; sweeps=[sweep_C6C12]}
301     directive data [R33S175_EYFP_ECFP]
302     drR33S175:device
303 }
304
305 // Timed additions circuit (for prediction)
306 system doublereceiverTimed = { R33S175 with directive parameters [ sigma = 1.0 ] }
307
308 // Relays
309 system R33S175_P76_growth = { growth with
310     directive simulation {multicore=True; sweeps=[sweep_relays]}
311     directive data [R33S175_P76LasI_OD]
312 }
313
314 system R33S175_P76_control = { control with
315     directive simulation {multicore=True; sweeps=[sweep_relays]}
316     directive data [R33S175_P76LasI_mRFP1]
317 }
318 system R33S175_P76 = { R33S175 with
319     directive simulation {multicore=True; sweeps=[sweep_relays]}
320     directive data [R33S175_P76LasI_EYFP_ECFP]
321     relayP76LasI:device
322 }
323
324 system R33S175_P81_growth = { growth with
325     directive simulation {multicore=True; sweeps=[sweep_relays]}
326     directive data [R33S175_P81LuxI_OD]
327 }
328
329 system R33S175_P81_control = { control with

```

```

330     directive simulation {multicore=True; sweeps=[sweep_relays]}
331     directive data [R33S175_P81LuxI_mRFP1]
332 }
333 system R33S175_P81 = { R33S175 with
334     directive simulation {multicore=True; sweeps=[sweep_relays]}
335     directive data [R33S175_P81LuxI_EYFP_ECFP]
336     relayP81LuxI:device
337 }
338
339 // PBad - Inducer
340 system PBADYFP = { target with
341     directive simulation { final=36.0; points=250; plots=[[x]*([yfp]+[f530])+b530];
342         plotcolours=["#FFDF00"]; multicore=True; sweeps=[sweep_PBAD_eYFP] }
343     directive parameters [
344         r = 1, { interval=Real; distribution=Uniform(0.1,10); variation=Multiple };
345         K = 2, { interval=Real; distribution=Uniform(0.1,5); variation=Multiple };
346         tlag = 1, { interval=Real; distribution=Uniform(0,10); variation=Multiple };
347         rc=1e2, { distribution=Uniform(1e0,1e5); variation=Multiple };
348         aYFP=1.0, { distribution=Uniform(1e0,1e5) };
349         b530=1e3, { interval=Real; distribution=Uniform(0.0,5e3) };
350     ]
351     directive data [PBAD_eYFP_EYFP]
352     pBADYFP:device
353 }
354
355 // AiiA - Degradable
356 system R33S175_PBADAiiA = { R33S175 with
357     directive simulation {multicore=True; sweeps=[sweep_R33S175_PBADAiiA]}
358     directive deterministic {reltolerance=1e-12; abstolerance=1e-10}
359     directive data [R33S175_PBADAiiA_EYFP_ECFP]
360     | pBADAiiA:device
361 }
362
363 // Auto
364 node Auto_Growth { systems = [auto_growth]; inference = {partial=true} }
365 node Auto_Control { systems = [auto_control]; inference = {partial=true} }
366 node Auto { systems = [auto] }
367 edge Auto_Growth.auto_growth ->[r=Fixed;K=Fixed;tlag=Fixed] Auto_Control.auto_control
368 edge Auto_Control.auto_control ->[r=Fixed;K=Fixed;tlag=Fixed;rc=Fixed] Auto.auto
369
370 // PRPR - Constitutive
371 node Constitutive_Growth { systems = [prpr_growth]; inference = {partial=true} }
372 node Constitutive_Control { systems = [prpr_control]; inference = {partial=true} }
373 node Constitutive { systems = [prpr] }
374 edge Constitutive_Growth.prpr_growth ->[r=Fixed;K=Fixed;tlag=Fixed]
375     Constitutive_Control.prpr_control
376 edge Constitutive_Control.prpr_control ->[r=Fixed;K=Fixed;tlag=Fixed;rc=Fixed] Constitutive.prpr
377 edge Auto_Control ->[dRFP] Constitutive_Control
378 edge Auto ->[a530;a480] Constitutive
379
380 // Receivers
381 node Receivers_Growth { systems = [PCat_growth; R100S32_growth; R33S32_growth; R33S175_growth];
382     inference = {partial=true} }
383 node Receivers_Control { systems = [PCat_control; R100S32_control; R33S32_control;
384     R33S175_control]; inference = {partial=true} }
385 node Receivers { systems = [PCat; R100S32; R33S32; R33S175] }
386 edge Receivers_Growth.PCat_growth ->[r=Fixed;K=Fixed;tlag=Fixed] Receivers_Control.PCat_control
387 edge Receivers_Growth.R100S32_growth ->[r=Fixed;K=Fixed;tlag=Fixed]
388     Receivers_Control.R100S32_control

```

```

384 edge Receivers_Growth.R33S32_growth ->[r=Fixed;K=Fixed;tlag=Fixed] Receivers_Control.R33S32_control
385 edge Receivers_Growth.R33S175_growth ->[r=Fixed;K=Fixed;tlag=Fixed]
    Receivers_Control.R33S175_control
386 edge Receivers_Control.PCat_control ->[r=Fixed;K=Fixed;tlag=Fixed;rc=Fixed] Receivers.PCat
387 edge Receivers_Control.R100S32_control ->[r=Fixed;K=Fixed;tlag=Fixed;rc=Fixed] Receivers.R100S32
388 edge Receivers_Control.R33S32_control ->[r=Fixed;K=Fixed;tlag=Fixed;rc=Fixed] Receivers.R33S32
389 edge Receivers_Control.R33S175_control ->[r=Fixed;K=Fixed;tlag=Fixed;rc=Fixed] Receivers.R33S175
390 edge Constitutive_Control ->[dRFP] Receivers_Control
391 edge Constitutive ->[a530; a480; dYFP; dCFP] Receivers
392
393 // Relays
394 node Relays_Growth { systems = [R33S175_P76_growth; R33S175_P81_growth]; inference =
    {partial=true} }
395 node Relays_Control { systems = [R33S175_P76_control; R33S175_P81_control]; inference =
    {partial=true} }
396 node Relays { systems = [R33S175_P76; R33S175_P81] }
397 edge Relays_Growth.R33S175_P76_growth ->[r=Fixed;K=Fixed;tlag=Fixed]
    Relays_Control.R33S175_P76_control
398 edge Relays_Growth.R33S175_P81_growth ->[r=Fixed;K=Fixed;tlag=Fixed]
    Relays_Control.R33S175_P81_control
399 edge Relays_Control.R33S175_P76_control ->[r=Fixed;K=Fixed;tlag=Fixed;rc=Fixed] Relays.R33S175_P76
400 edge Relays_Control.R33S175_P81_control ->[r=Fixed;K=Fixed;tlag=Fixed;rc=Fixed] Relays.R33S175_P81
401 edge Receivers_Control ->[dRFP] Relays_Control
402 edge Receivers ->[
403     a530;a480;dYFP;dCFP;
404     aR33;aS175;aYFP;aCFP;e76;e81;KGR_76;KGS_76;KGR_81;KGS_81;KR6;KS6;KR12;KS12;nR;nS;dR;
405 ] Relays
406
407 // PBad - Inducer
408 node Inducer_Growth { systems = [growth]; inference = {partial=true} }
409 node Inducer_Control { systems = [control]; inference = {partial=true} }
410 node Inducer { systems = [PBADYFP] }
411 edge Inducer_Growth.growth ->[r=Fixed;K=Fixed;tlag=Fixed] Inducer_Control.control
412 edge Inducer_Control.control ->[r=Fixed;K=Fixed;tlag=Fixed;rc=Fixed] Inducer.PBADYFP
413 edge Constitutive_Control ->[dRFP] Inducer_Control
414 edge Constitutive ->[a530;dYFP] Inducer
415
416 // AiiA - Degradar
417 node Degradar_Growth { systems = [growth]; inference = {partial=true} }
418 node Degradar_Control { systems = [control]; inference = {partial=true} }
419 node Degradar { systems = [R33S175_PBADAiiA] }
420 edge Degradar_Growth.growth ->[r=Fixed;K=Fixed;tlag=Fixed] Degradar_Control.control
421 edge Degradar_Control.control ->[r=Fixed;K=Fixed;tlag=Fixed;rc=Fixed] Degradar.R33S175_PBADAiiA
422 edge Receivers_Control ->[dRFP] Degradar_Control
423 edge Receivers ->[
424     a530;a480;dYFP;dCFP;
425     aR33;aS175;aYFP;aCFP;e76;e81;KGR_76;KGS_76;KGR_81;KGS_81;KR6;KS6;KR12;KS12;nR;nS;dR;
426 ] Degradar
427 edge Inducer ->[Kara; nA; eA] Degradar

```

S2 Models of cells expressing synthetic gene circuits

This section explains the models of the cell lines that were built and tested for the Constant hypothesis. Each subsection focuses on a system specified in the code in Listing 1. For the sake of convenience and readability, we have unrolled (expanded) the systems to be a self-contained system definition. Tables S2 and S3 list the parts and devices that were built, tested, and used in this case study.

S2.1 No plasmid (Autofluorescence)

The simplest possible cell line to characterize is one in which there is no synthetic gene circuit at all. However, applying dynamic characterization to no circuit is useful to characterize how autofluorescence depends on cell density and gene expression capacity. Therefore, our chromosomal RFP-expressing cells were measured under a range of conditions, to explore how gene expression capacity influenced time-series measurements at fluorescence wavelengths corresponding to eYFP and eCFP .

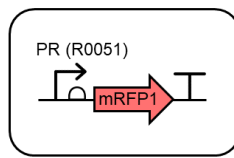


Figure S2: Design of chromosomal RFP.

Model definition

The model we used for autofluorescence assumes that the rate of autofluorescence is proportional to gene expression capacity, $h(c)$, and that the fluorescent material dilutes with cell growth. Bulk autofluorescence is then quantified in exactly the same way as it is when there is a synthetic gene circuit inside the cells, using equation (4) of the main text. As such, the equations for intracellular autofluorescence corresponding to eYFP and eCFP are

$$\frac{dc}{dt} = \gamma(c).c \quad (\text{S1a})$$

$$\frac{d[F_{530}]}{dt} = a_{530}.h(c) - \gamma(c)[F_{530}] \quad (\text{S1b})$$

$$\frac{d[F_{480}]}{dt} = a_{480}.h(c) - \gamma(c)[F_{480}] \quad (\text{S1c})$$

To compare with experimental measurements, we consider the bulk fluorescence given by

$$B_{480} = c.[F_{480}] + b_{480} \quad (\text{S2a})$$

$$B_{530} = c.[F_{530}] + b_{530} \quad (\text{S2b})$$

where $[F_{480}]$ and $[F_{530}]$ are modeled as in (14). This is equivalent to the observer process described in the Methods section, but with $[YFP]$ and $[CFP]$ set to zero, as they are not expressed in this circuit.

Implementation with GEC/CRN language

To implement the combination of modeling cell density and autofluorescence in the GEC language, we define a module that can be called as part of the implementation of any other circuit. We also use *rate* expressions to define γ (growth) and $h(c)$ (capacity, here the TargetSwitch hypothesis), as these are reused in multiple reactions across different modules/systems.

```
1 directive rates [
2   growth = [grow]*r*(1 - [x] / K);
```

```

3   capacity = rc;
4 ]
5 module cells(growth,tlag) = {
6   init x c0 | init grow 1 @ tlag |
7   init c6 C6 @ tau | init c12 C12 @ tau |
8   ->[[growth]*[x]] x
9 }
10 module autofluorescence(growth,capacity) = {
11   ->[[capacity]*a530] f530 |
12   f530 ->[[growth]*[f530]] |
13   ->[[capacity]*a480] f480 |
14   f480 ->[[growth]*[f480]]
15 }

```

Characterization experiment

We infer the Auto model parameters by using uniform priors on a_{530} , a_{480} , b_{530} , b_{480} and any parameters that are specific to the gene expression capacity hypothesis being considered. The parameters within γ are taken to be the maximum likelihood estimates from the cell density characterization phase, and the ζ are either taken to be the maximum likelihood estimates from the control characterization phase or are inferred within the target phase, depending on the hypothesis in question.

According, the overall model for the Auto circuit is simply that instantiation of the `cells` module above, along with the specification of the parameters to be inferred:

```

1 system auto = {
2   directive simulation { final=36.0; points=250; plots=[[x]*[f530]+b530; [x]*[f480]+b480];
3     plotcolours=["#FFDF00"; "#ADD8E6"] }
4   directive parameters [
5     r = 1, { interval=Real; distribution=Uniform(0.1,10); variation=Multiple };
6     K = 2, { interval=Real; distribution=Uniform(0.1,5); variation=Multiple };
7     tlag = 1, { interval=Real; distribution=Uniform(0,10); variation=Multiple };
8     rc=1e2, { interval=Log; distribution=Uniform(1e0,1e5); variation=Multiple };
9     b530=1e3, { interval=Real; distribution=Uniform(0.0,5e3); variation=Random };
10    b480=1e3, { interval=Real; distribution=Uniform(0.0,1e4); variation=Random };
11  ]
12  directive rates [growth = [grow]*r*(1 - [x] / K);capacity = rc]
13  directive crn { cells(growth,tlag) | autofluorescence(growth,capacity) }

```

Characterization results

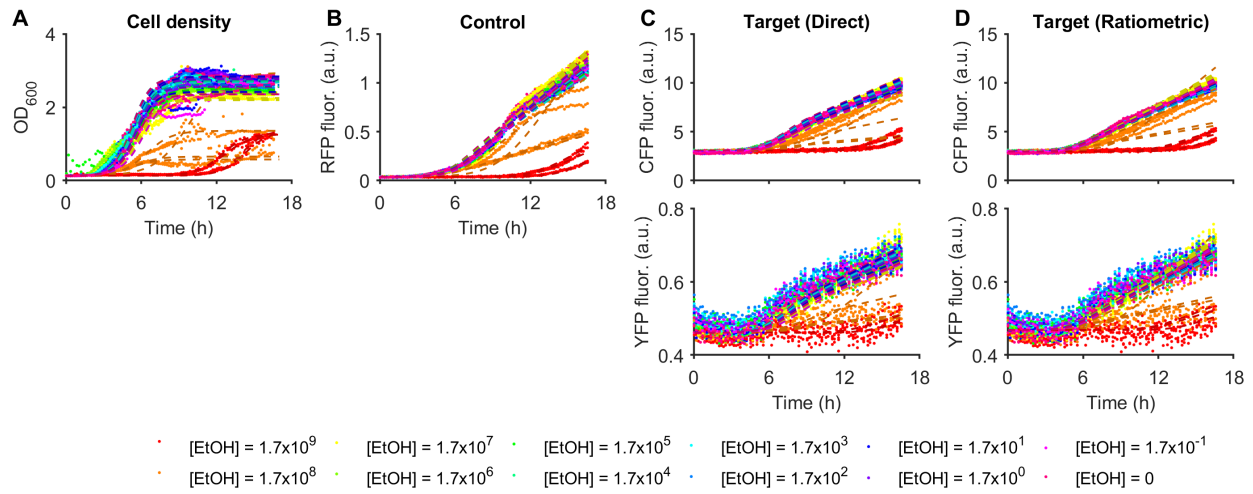
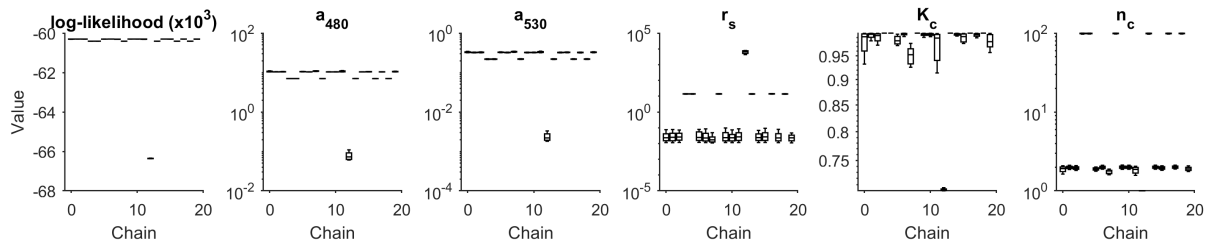
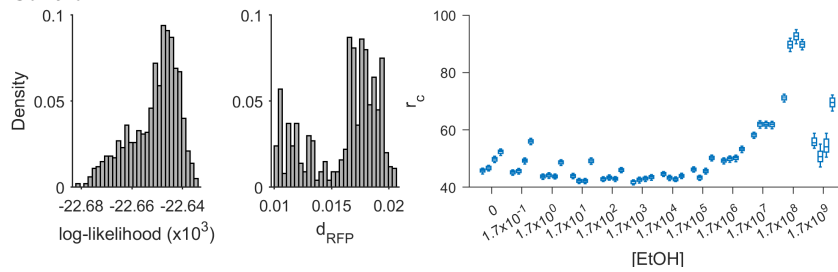


Figure S3: Model-data comparison for the Auto circuit with TargetSwitch hypothesis. Measurements of the Auto circuit are compared against simulations of the maximum likelihood parameter set from the TargetSwitch hypothesis.

A Direct



B Control



C Ratiometric

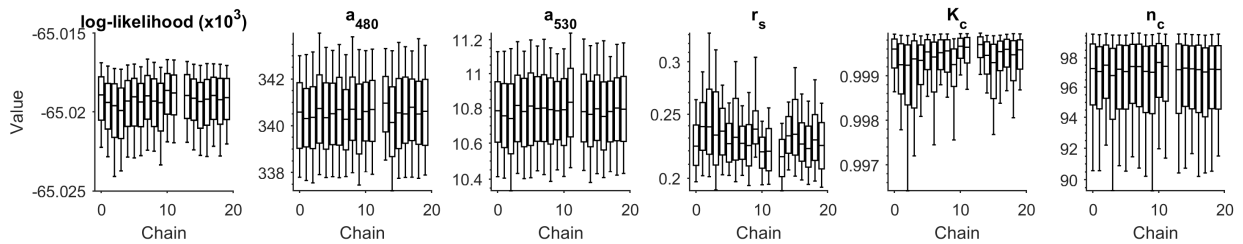


Figure S4: Marginal parameter posterior distributions for Auto with TargetSwitch hypothesis. A. Inference of circuit parameters using the direct (non-ratiometric) method, which corresponds to assuming that $r_c = 1$ for all time-series traces. **B.** The control phase identifies values for r_c for each time-series, to be used in ratiometric characterization. **C.** Inference of circuit parameters using the ratiometric method, using the values of r_c in B.

S2.2 Constitutive expression via the PR promoter

The simplest circuit that we consider in this article uses constitutive promoters to drive expression of eYFP and eCFP . Using such a simple circuit enables us to characterize properties of the fluorescent proteins, which can then be reused in to aide characterization of circuits using the same fluorescent proteins.

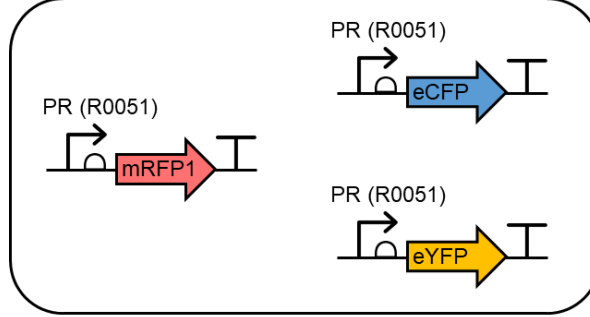
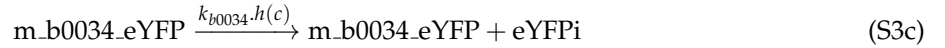


Figure S5: Design of constitutive expression circuit.

Model definition

As this is the first (non-trivial) synthetic gene circuit that we describe, we include a detailed derivation. We start by considering the chemical reactions introduced by the circuit in Fig. S5.

If we denote by g the plasmid containing the PL:eYFP and PL:eCFP cassettes, then we can write a system of chemical reactions that describe transcription, translation and fluorescent protein maturation as



where $h(c)$ is the gene expression capacity, as introduced in the Methods section of the main text.

Translating to ODEs, and replacing $[g]$ with N , the plasmid copy number, we obtain

$$\frac{dc}{dt} = \gamma(c).c \quad (\text{S4a})$$

$$\frac{d[\text{m.b0034.eYFP}]}{dt} = a_{r0011}.N - (d_{\text{m.b0034.eYFP}} + \gamma(c))[\text{m.b0034.eYFP}] \quad (\text{S4b})$$

$$\frac{d[\text{eYFPi}]}{dt} = k_{b0034}.h(c).[\text{m.b0034.eYFP}] - (d_{\text{YFP}} + \mu_{\text{YFP}} + \gamma(c))[\text{eYFP}] \quad (\text{S4c})$$

$$\frac{d[\text{eYFP}]}{dt} = \mu_{\text{YFP}}[\text{eYFPi}] - (d_{\text{YFP}} + \gamma(c))[\text{eYFP}] \quad (\text{S4d})$$

$$\frac{d[\text{m.b0034.eCFP}]}{dt} = a_{r0011}.N - d_{\text{m.b0034.eCFP}}[\text{m.b0034.eCFP}] \quad (\text{S4e})$$

$$\frac{d[\text{eCFPi}]}{dt} = k_{b0034}.h(c).[\text{m.b0034.eCFP}] - (d_{\text{CFP}} + \mu_{\text{CFP}} + \gamma(c))[\text{eCFPi}] \quad (\text{S4f})$$

$$\frac{d[\text{eCFP}]}{dt} = \mu_{\text{CFP}}[\text{eCFPi}] - (d_{\text{CFP}} + \gamma(c))[\text{eCFP}] \quad (\text{S4g})$$

where $\gamma(c)$ is the cellular dilution of each molecular concentration.

Assumption 1: By assuming that mRNA dynamics are fast, we can remove the mRNA species from the model entirely. That is, we equate (S4b) and (S4e) to zero, solve for $[\text{m.b0034.eYFP}]$ and $[\text{m.b0034.eCFP}]$, and then substitute into the remaining equations. This results in the reduced model

$$\frac{dc}{dt} = \gamma(c).c \quad (\text{S5a})$$

$$\frac{d[\text{eYFPi}]}{dt} = a_{\text{YFP}}.h(c) - (d_{\text{YFP}} + \mu_{\text{YFP}} + \gamma(c))[\text{eYFP}] \quad (\text{S5b})$$

$$\frac{d[\text{eYFP}]}{dt} = \mu_{\text{YFP}}[\text{eYFPi}] - (d_{\text{YFP}} + \gamma(c))[\text{eYFP}] \quad (\text{S5c})$$

$$\frac{d[\text{eCFPi}]}{dt} = a_{\text{CFP}}.h(c) - (d_{\text{CFP}} + \mu_{\text{CFP}} + \gamma(c))[\text{eCFPi}] \quad (\text{S5d})$$

$$\frac{d[\text{eCFP}]}{dt} = \mu_{\text{CFP}}[\text{eCFPi}] - (d_{\text{CFP}} + \gamma(c))[\text{eCFP}] \quad (\text{S5e})$$

where

$$a_{\text{YFP}} = \frac{a_{r0011}.N.k_{b0034}}{d_{\text{m.b0034.eYFP}} + \gamma(c)} \approx \frac{a_{r0011}.N.k_{b0034}}{d_{\text{m.b0034.eYFP}}}, \quad a_{\text{CFP}} = \frac{a_{r0011}.N.k_{b0034}}{d_{\text{m.b0034.eCFP}} + \gamma(c)} \approx \frac{a_{r0011}.N.k_{b0034}}{d_{\text{m.b0034.eCFP}}} \quad (\text{S6})$$

Here, we remove $\gamma(c)$ from the denominator because dilution will normally be slower than mRNA degradation, and making this simplification results in a_{YFP} and a_{CFP} being constant. Finally, we note here that despite simplifying the parametrization (removing a_{r0011} , k_{b0034} , $d_{\text{m.b0034.eYFP}}$ and $d_{\text{m.b0034.eCFP}}$), we should keep in mind that there is a dependency of a_{YFP} and a_{CFP} on the biological parts in each cassette.

Assumption 2: By assuming that fluorescent protein maturation is fast, we can remove the equations for the concentration of immature fluorescent proteins. Let $[\text{YFP}]$ be the sum of the concentrations of immature and mature fluorescent proteins. Adding (S5b) to (S5c), we obtain

$$\begin{aligned} \frac{d}{dt} ([\text{eYFPi}] + [\text{eYFP}]) &= a_{\text{YFP}}.h(c) - (d_{\text{YFP}} + \gamma(c)) ([\text{eYFPi}] + [\text{eYFP}]) \\ \implies \frac{d[\text{YFP}]}{dt} &= a_{\text{YFP}}.h(c) - (d_{\text{YFP}} + \gamma(c))[\text{YFP}] \end{aligned} \quad (\text{S7})$$

and similarly for eCFP. If we assume that the immature form is instantly converted to the mature form, then the concentration of the mature form is equal to the total concentration. Therefore, the resultant system

of equations is given by

$$\frac{dc}{dt} = \gamma(c).c \quad (\text{S8a})$$

$$\frac{d[\text{YFP}]}{dt} = a_{\text{YFP}}.h(c) - (d_{\text{YFP}} + \gamma(c))[\text{YFP}] \quad (\text{S8b})$$

$$\frac{d[\text{CFP}]}{dt} = a_{\text{CFP}}.h(c) - (d_{\text{CFP}} + \gamma(c))[\text{CFP}] \quad (\text{S8c})$$

We compare with experimental measurements using the observer process of (4).

Implementation with GEC/CRN language

To implement the PRPR circuit in the GEC language, we define modules for the eYFP and eCFP proteins, we can then be called by multiple systems (note that module definitions are identical in both GEC and CRN). We require an argument P for the normalized promoter activity (rate expression) and another argument a for the maximal production rate. This enables circuits that use different promoters or ribosome binding sites for eYFP and eCFP to provide different contexts in the module call. The rate expressions `growth` and `capacity` are used equivalently to the Auto circuit.

```

1 module CFP(P,a,growth,capacity) = {
2   ->[[capacity]*a*[P]] cfp |
3   cfp ->{dCFP} |
4   cfp ->[[growth]*[cfp]]
5 }
6 module YFP(P,a,growth,capacity) = {
7   ->[[capacity]*a*[P]] yfp |
8   yfp ->{dYFP} |
9   yfp ->[[growth]*[yfp]]
10 }
11 device prpr() = { YFP(one,aYFP,growth,capacity) | CFP(one,aCFP,growth,capacity) }
```

It's also important to note that this code has incorporated the assumptions above concerning fluorescent protein maturation and mRNA expression. Alternative assumptions can simply be explored in this framework but modifying these module definitions.

Characterization experiment

We measured the PRPR circuit in response to varying concentrations of chloramphenicol, an inhibitor of protein translation. By inhibiting protein translation, we directly alter the gene expression capacity term in our models, enabling us to test whether $h(c)$ can capture such an effect implicitly. Unfortunately, chloramphenicol also considerably alters cell growth, so separating its effects on cell growth and gene expression is a challenge to the methods we are demonstrating in this paper.

We infer the PRPR model parameters by using (uninformative) uniform priors on the previously uncharacterized parameters a_{CFP} , a_{YFP} , d_{CFP} and d_{YFP} , and (informative) truncated Gaussian priors on a_{480} and a_{530} , with mean and standard deviation taken from the marginal posteriors of the Auto circuit characterization. These parameters are globally specified, with propagation of marginal posteriors as edges of the inference graph (see Listing 1). We also use uninformative priors on the background fluorescence parameters (specified below as local parameters `b480` and `b530`), without propagating their marginal posteriors from previous circuits.

In the GEC language, the overall model for the PRPR circuit combines instantiation of the `cells` and `autofluorescence` modules and the `prpr` device. In the following system definition, a device invocation `prpr` implies that the system must use the device model definition `device prpr()`. The structural definition of the `prpr` device (specified in the GEC library and detailed in Table S3) is : `pr; rbs34; eyfp; ter1; pr; rbs34; ecfp; ter1`. The part definitions for these DNA components can be found in Table S2. This applies for all device invocations in systems in all the subsequent sections.

```

1 system prpr = {
2   directive simulation { final=36.0; points=250; plots=[[x]*([yfp]+[f530])+b530;
3     [x]*([cfp]+[f480])+b480]; plotcolours=["#FFDF00"; "#ADD8E6"] }
4   directive rates [growth = [grow]*r*(1 - [x] / K); capacity = rc]
5   directive crn { cells(growth,tlag) | autofluorescence(growth,capacity) }
6   directive parameters [
7     r = 1, { interval=Real; distribution=Uniform(0.1,10); variation=Multiple };
8     K = 2, { interval=Real; distribution=Uniform(0.1,5); variation=Multiple };
9     tlag = 1, { interval=Real; distribution=Uniform(0,10); variation=Multiple };
10    rc=1e2, { interval=Log; distribution=Uniform(1e0,1e5); variation=Multiple };
11    aCFP=1e3, { interval=Log; distribution=Uniform(1e0,1e5); variation=Random };
12    aYFP=1e3, { interval=Log; distribution=Uniform(1e0,1e5); variation=Random };
13    b530=1e3, { interval=Real; distribution=Uniform(0.0,5e3); variation=Random };
14    b480=1e3, { interval=Real; distribution=Uniform(0.0,1e4); variation=Random };
15  ]
16  prpr:device
17 }

```

Here, system-local parameters aCFP and aYFP replace the global parameters (see Listing 1). This is to enable the PR promoter in combination with the b0034 rbs to take on a different maximum production rate than the PLux-driven production rates of the other devices. The other important parameters for this device are dCFP and dYFP, and are globally specified (Listing 1).

Characterization results

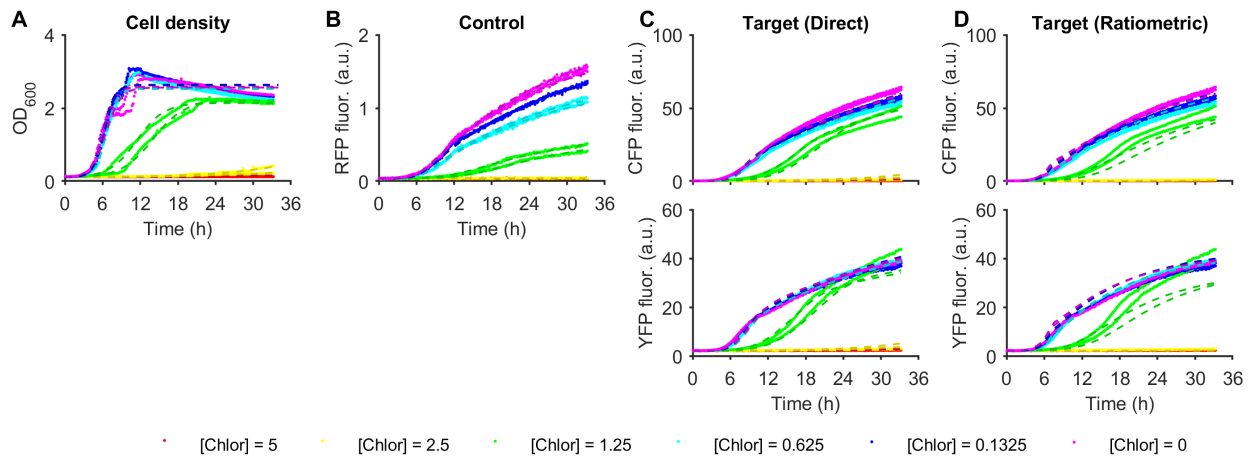


Figure S6: Model-data comparison for the PRPR circuit with TargetSwitch hypothesis. Measurements of the PRPR circuit are compared against simulations of the maximum likelihood parameter set from the TargetSwitch hypothesis.

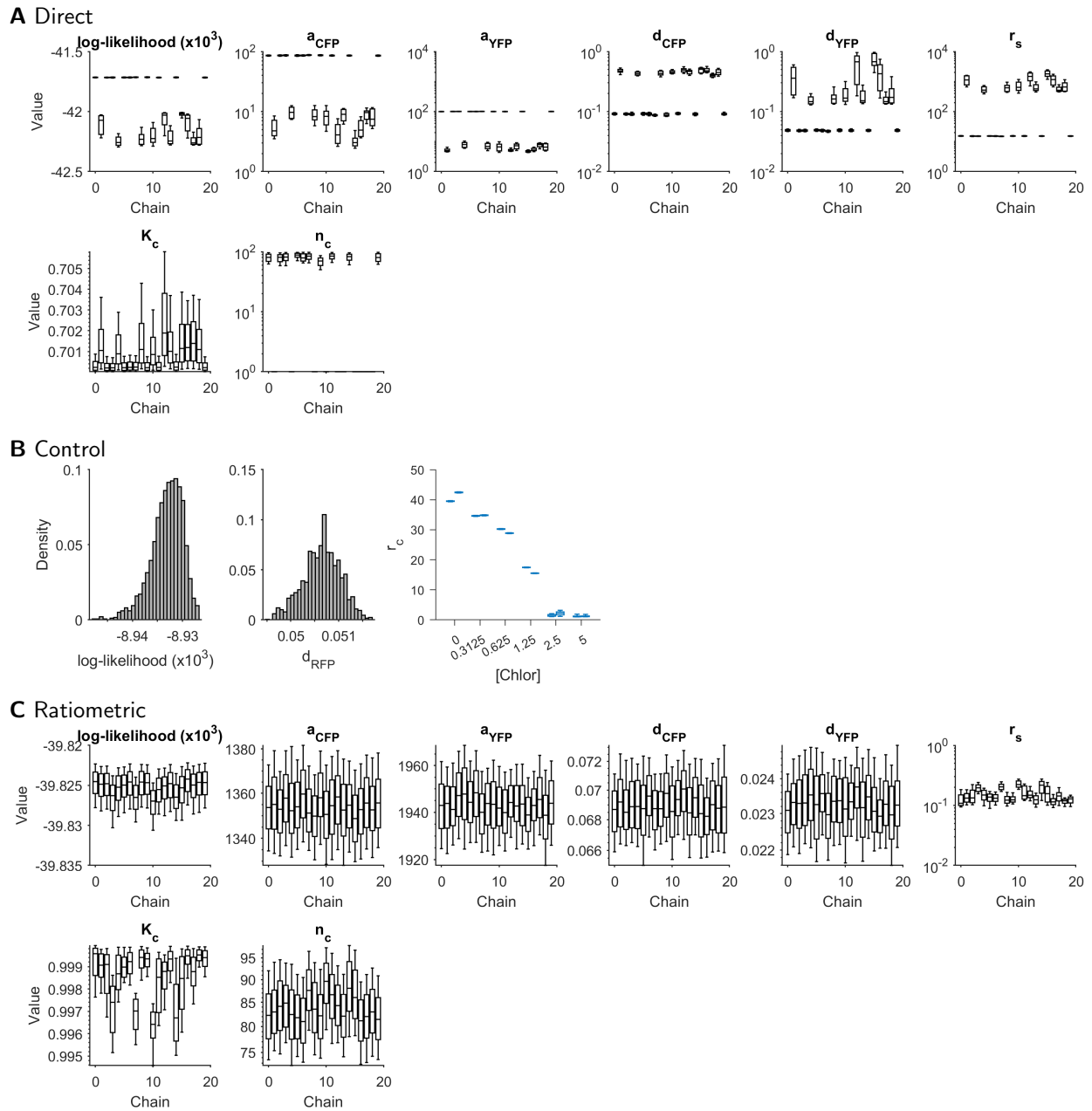


Figure S7: Marginal parameter posterior distributions for PRPR with TargetSwitch hypothesis. A. Inference of circuit parameters using the direct (non-ratiometric) method, which corresponds to assuming that $r_c = 1$ for all time-series traces. B. The control phase identifies values for r_c for each time-series, to be used in ratiometric characterization. C. Inference of circuit parameters using the ratiometric method, using the values of r_c in B.

S2.3 HSL Double Receivers

We consider the dynamic characterization of the AHL double receiver (DR) circuit introduced in [3]. In this device, two variations of the wild-type PLux promoter, PLux76 and PLas81, were engineered to bind preferentially to activated luxR and lasR complexes respectively. As LuxR favours binding of C6 and LasR favours binding of C12, optimized expression of LuxR and LasR can lead to near-orthogonal intracellular detection of C6 and C12. The double receiver device was originally measured with PLux76 upstream of the coding sequence for eCFP, and PLas81 upstream of the coding sequence for eYFP. A plasmid containing all of this machinery was then inserted into cells chromosomally expressing mRFP1, which could be used as a ratiometric control.

Model definition

As the modelling philosophy we are considering here describes dynamics of proteins, the model of DR circuits in this paper differs from model described previously [3], as the concentrations of luxR and lasR become dynamic quantities affected by growth dilution. Furthermore, in the previous paper, we parametrized the double receiver by first parametrizing circuits that only have one PLux promoter. Here, we seek to parametrize the DR circuits directly, by inferring parameters against eYFP and eCFP measurements simultaneously. As such, the model must consider that luxR and lasR-based regulators (bound to HSLs) might bind to more than one (PLux) promoter.

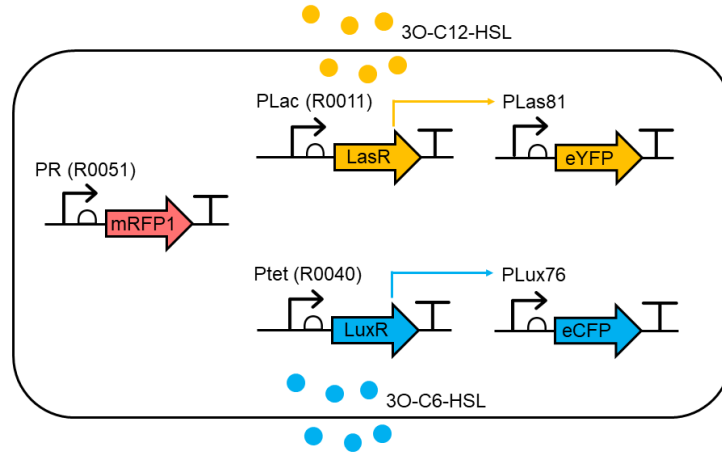
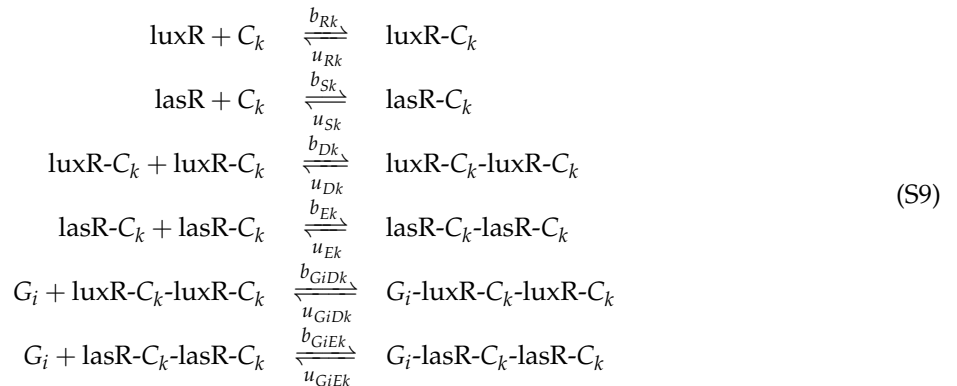


Figure S8: Design of a DR circuit.

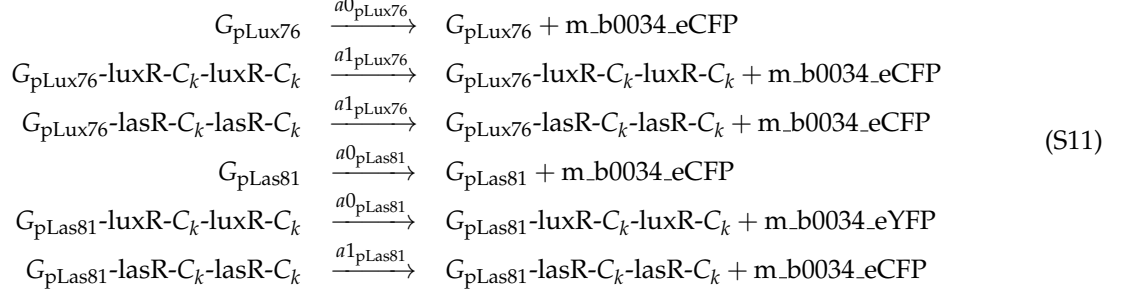
We denote by C_k the HSL molecule with length k carbon chain, and by G_i the PLux76 and PLas81 promoters. Then similar to the derivation in [3], we can specify all of the reactions between the HSLs, LuxR and LasR, and eventual binding of transcriptional regulators to PLux76/PLas81.



Constitutive expression of luxR, lasR is described by



Inducible expression of eCFP and eYFP by P_{OLux} and P_{OLas} respectively is described by



The full DR circuit comprises reactions (S9), (S10) and (S11), and the same reactions as shown for the PRPR circuit that describe mRNA translation for eCFP and eYFP .

To produce a simplified ODE model amenable to parameter inference, we start with the equations describing luxR and lasR protein, their complexes involving C₆ and C₁₂, and the bound/unbound promoters. Applying also Assumption 1 from before, we arrive a set of equations for the non-mRNA species as

$$\frac{dc}{dt} = \gamma(c) \cdot c \quad (\text{S12a})$$

$$\frac{d[\text{luxR}]}{dt} = a_R + u_{Rk}[\text{luxR-C}_k] - [\text{luxR}](\gamma(c) + d_R + b_{Rk}[C_k]) \quad (\text{S12b})$$

$$\frac{d[\text{lasR}]}{dt} = a_S + u_{Sk}[\text{lasR-C}_k] - [\text{lasR}](\gamma(c) + d_S + b_{Sk}[C_k]) \quad (\text{S12c})$$

$$\frac{d[\text{luxR-C}_k]}{dt} = b_{Rk}[\text{luxR}][C_k] + 2u_{Dk}[\text{luxR-C}_k\text{-luxR-C}_k] - [\text{luxR-C}_k](\gamma(c) + d_R^1 + u_{Rk} + 2b_{Dk}[\text{luxR-C}_k]) \quad (\text{S12d})$$

$$\frac{d[\text{lasR-C}_k]}{dt} = b_{Sk}[\text{lasR}][C_k] + 2u_{Ek}[\text{lasR-C}_k\text{-lasR-C}_k] - [\text{lasR-C}_k](\gamma(c) + d_S^1 + u_{Sk} + 2b_{Ek}[\text{lasR-C}_k]) \quad (\text{S12e})$$

$$\begin{aligned} \frac{d[\text{luxR-C}_k\text{-luxR-C}_k]}{dt} &= b_{Dk}[\text{luxR-C}_k]^2 + u_{GiDk} \sum_i [G_i\text{-luxR-C}_k\text{-luxR-C}_k] \dots \\ &\quad - [\text{luxR-C}_k\text{-luxR-C}_k] \left(\gamma(c) + d_R^1 + u_{Dk} + b_{GiDk} \sum_i [G_i] \right) \end{aligned} \quad (\text{S12f})$$

$$\begin{aligned} \frac{d[\text{lasR-C}_k\text{-lasR-C}_k]}{dt} &= b_{Ek}[\text{lasR-C}_k]^2 + u_{GiEk} \sum_i [G_i\text{-lasR-C}_k\text{-lasR-C}_k] \dots \\ &\quad - [\text{lasR-C}_k\text{-lasR-C}_k] \left(\gamma(c) + d_S^1 + u_{Ek} + b_{GiEk} \sum_i [G_i] \right) \end{aligned} \quad (\text{S12g})$$

$$\frac{d[G_i\text{-luxR-C}_k\text{-luxR-C}_k]}{dt} = b_{GiDk}[G_i][\text{luxR-C}_k\text{-luxR-C}_k] - (\gamma(c) + u_{GiDk})[G_i\text{-luxR-C}_k\text{-luxR-C}_k] \quad (\text{S12h})$$

$$\frac{d[G_i\text{-lasR-C}_k\text{-lasR-C}_k]}{dt} = b_{GiEk}[G_i][\text{lasR-C}_k\text{-lasR-C}_k] - (\gamma(c) + u_{GiEk})[G_i\text{-lasR-C}_k\text{-lasR-C}_k] \quad (\text{S12i})$$

$$\begin{aligned} \frac{d[G_i]}{dt} &= \gamma(c) \cdot n_G + u_{GiDk}[G_i\text{-luxR-C}_k\text{-luxR-C}_k] + u_{GiEk}[G_i\text{-lasR-C}_k\text{-lasR-C}_k] \dots \\ &\quad - [G_i](\gamma(c) + b_{GiDk}[\text{luxR-C}_k\text{-luxR-C}_k] + b_{GiEk}[\text{lasR-C}_k\text{-lasR-C}_k]) \end{aligned} \quad (\text{S12j})$$

Here, luxR-C_k refers to a luxR-HSL heterodimer and luxR-C_k-luxR-C_k is the tetramer comprising two luxR-C_k complexes (no cross-binding of C₆ and C₁₂ dimers). Similarly, lasR-C_k and lasR-C_k-lasR-C_k are equivalent

lasR-HSL complexes. The luxR and lasR proteins are assumed to be stabilized by the binding of signal, as in [4]. Therefore, rates $d_j^1 < d_j$ ($j = R, S$) are the slower rates for signal-bound luxR/lasR proteins.

Solving most of the above system equal to zero, we obtain the quasi-equilibrium

$$[G_i\text{-luxR-C}_k\text{-luxR-C}_k]^* = K_{GDk}[G_i][\text{luxR-C}_k\text{-luxR-C}_k] \quad (\text{S13a})$$

$$[\text{luxR-C}_k\text{-luxR-C}_k]^* = K_{Dk}[\text{luxR-C}_k]^2 \quad (\text{S13b})$$

$$[\text{luxR-C}_k]^* = K_{Rk}[\text{luxR}][C_k] \quad (\text{S13c})$$

where $K_{Rk} = \frac{b_{Rk}}{\gamma + u_{Rk}}$, $K_{Dk} = \frac{b_{Dk}}{u_{Dk}}$ and $K_{GiDk} = \frac{b_{GiDk}}{u_{GiDk}}$. Therefore (also symmetry of luxR and lasR),

$$[G_i\text{-luxR-C}_k\text{-luxR-C}_k]^* = K_{GiDk}K_{Dk}(K_{Rk}[C_k][\text{luxR}])^2 \quad (\text{S14a})$$

$$[G_i\text{-lasR-C}_k\text{-lasR-C}_k]^* = K_{GiEk}K_{Ek}(K_{Sk}[C_k][\text{lasR}])^2 \quad (\text{S14b})$$

where the new K 's are defined as above.

In the reduced system, total luxR is described by the equations

$$\frac{d[\text{luxR}]_T}{dt} = \frac{d[\text{luxR}]}{dt} + \sum_k \left(\frac{d[\text{luxR-C}_k]}{dt} + 2 \frac{d[\text{luxR-C}_k\text{-luxR-C}_k]}{dt} + 2 \sum_i \frac{d[G_i\text{-luxR-C}_k\text{-luxR-C}_k]}{dt} \right) \quad (\text{S15a})$$

$$= a_R - \gamma[\text{luxR}] - d_R[\text{luxR}] \dots$$

$$- \sum_k \left((\gamma + d_R^1)[\text{luxR-C}_k] + (\gamma + d_R^1)[\text{luxR-C}_k\text{-luxR-C}_k] + \gamma \sum_i [G_i\text{-luxR-C}_k\text{-luxR-C}_k] \right) \quad (\text{S15b})$$

$$= a_R - \gamma[\text{luxR}]_T - d_R^1[\text{luxR}]_T - (d_R - d_R^1)[\text{luxR}] \quad (\text{S15c})$$

The final term needs careful attention, as we expect a difference between d_R and d_R^1 . Nevertheless, the obvious approximation is to ignore this difference, and model $[\text{luxR}]_T$ explicitly with no dependence on $[R]$. We can write down expressions for the fraction of $[\text{luxR}]_T$ that is bound to signal, dimerized, etc., using the equilibrium relationships above. E.g.

$$\begin{aligned} [\text{luxR}]_T &= [\text{luxR}] + \sum_k \left([\text{luxR-C}_k] + 2[\text{luxR-C}_k\text{-luxR-C}_k] + 2 \sum_i [G_i\text{-luxR-C}_k\text{-luxR-C}_k] \right) \\ &= [\text{luxR}] + \sum_k \left(K_{Rk}[\text{luxR}][C_k] + 2K_{Dk}K_{Rk}^2[\text{luxR}]^2[C_k]^2 + \sum_i 2K_{GiDk}[G_i]K_{Dk}K_{Rk}^2[\text{luxR}]^2[C_k]^2 \right) \end{aligned}$$

When C_k is low, total LuxR is closely approximated by free LuxR, $[\text{luxR}]_T \approx [\text{luxR}]$. But when C_k is high, $[\text{luxR}]_T$ should be partitioned between the $[\text{luxR-C}_k\text{-luxR-C}_k]$ and $[G_i\text{-luxR-C}_k\text{-luxR-C}_k]$ species. Therefore, to simplify the analysis, we propose modelling this by using the assumption

$$[\text{luxR}]_T \approx [\text{luxR}] + \sum_k [\text{luxR-C}_k] = [\text{luxR}] \left(1 + \sum_k K_{Rk}[C_k] \right) \quad (\text{S16})$$

which still captures the saturation of luxR by C_k , using the approximations

$$[\text{luxR}] \approx [\text{luxR}]_T \cdot \frac{1}{1 + \sum_k K_{Rk}[C_k]} \quad (\text{S17a})$$

$$[\text{luxR-C}_k] \approx [\text{luxR}]_T \cdot \frac{K_{Rk}[C_k]}{1 + \sum_k K_{Rk}[C_k]} \quad (\text{S17b})$$

$$[\text{luxR-C}_k\text{-luxR-C}_k] \approx K_{Dk}[\text{luxR}]_T^2 \left(\frac{K_{Rk}[C_k]}{1 + \sum_k K_{Rk}[C_k]} \right)^2 \quad (\text{S17c})$$

$$[G_i\text{-luxR-C}_k\text{-luxR-C}_k] \approx K_{GR}^{(i)}[G_i][\text{luxR}]_T^2 \left(\frac{K_{Rk}[C_k]}{1 + \sum_k K_{Rk}[C_k]} \right)^2 \quad (\text{S17d})$$

where $K_{GR}^{(i)} = K_{GiDk}K_{Dk}$ is assumed to be independent of which signal is bound (k), equivalent to the derivation in [3].

The approximation also allows for saturation of G_i . By taking advantage of the conservation law $[G_i] + [G_i.\text{luxR}-C_6-\text{luxR}-C_6] + [G_{12}-\text{luxR}-C_1-\text{luxR}-C_1] + [G_6-\text{lasR}-C_1-\text{lasR}-C_1] + [G_{12}-\text{lasR}-C_1-\text{lasR}-C_1] = N_i$, we can derive the rate of production of mRNA as a function of $[R]_T$, $[S]_T$, $[C_6]$ and $[C_{12}]$. For notational convenience we drop the square brackets and T subscript, which allows us to write

$$f_i(R, S, C_6, C_{12}) = \frac{e^{(i)} + K_{GR}^{(i)} R^2 \left(\frac{K_{Rk} C_k}{1 + \sum_k K_{Rk} C_k} \right)^{n_R} + K_{GS}^{(i)} S^2 \left(\frac{K_{Sk} C_k}{1 + \sum_k K_{Sk} C_k} \right)^{n_S}}{1 + K_{GR}^{(i)} R^2 \left(\frac{K_{Rk} C_k}{1 + \sum_k K_{Rk} C_k} \right)^{n_R} + K_{GS}^{(i)} S^2 \left(\frac{K_{Sk} C_k}{1 + \sum_k K_{Sk} C_k} \right)^{n_S}} \quad (\text{S18})$$

where $K_{G_i-\text{luxR}}$ and $K_{G_i-\text{lasR}}$ are scaled to incorporate K_{Dk} and K_{Ek} respectively, and we introduce alternative exponents n_R and n_S , analogous to the usage of n in [3]. Accordingly, we obtain the following system of equations

$$\frac{dc}{dt} = \gamma(c).c \quad (\text{S19a})$$

$$\frac{d[\text{luxR}]}{dt} = a_R.h(c) - (d_R + \gamma(c))[\text{luxR}] \quad (\text{S19b})$$

$$\frac{d[\text{lasR}]}{dt} = a_S.h(c) - (d_R + \gamma(c))[\text{lasR}] \quad (\text{S19c})$$

$$\frac{d[\text{CFP}]}{dt} = a_{\text{CFP}}.h(c).f_{76}([C_6], [C_{12}], [R], [S]) - (d_{\text{CFP}} + \gamma(c))[\text{CFP}] \quad (\text{S19d})$$

$$\frac{d[\text{YFP}]}{dt} = a_{\text{YFP}}.h(c).f_{81}([C_6], [C_{12}], [R], [S]) - (d_{\text{YFP}} + \gamma(c))[\text{YFP}] \quad (\text{S19e})$$

where the variables R and S now represent total luxR and lasR respectively, and γ is as defined in (6).

Implementation with GEC/CRN language

The DR circuit introduces expression of LuxR and LasR proteins, so we define modules for their synthesis, taking the same strategy as done for eYFP /eCFP in the PRPR circuit above. However, as we only use the same promoters across all circuits in this paper, and they are used in a non-inducible way, there is no need to have a rate expression that multiplies the overall expression rate.

```

1 module LuxR(aR,growth,capacity) = {
2   ->[[capacity]*aR] luxR |
3   luxR ->{dR} |
4   luxR ->[[growth]*[luxR]]
5 }
6 module LasR(aS,growth,capacity) = {
7   ->[[capacity]*aS] lasR |
8   lasR ->{dR} |
9   lasR ->[[growth]*[lasR]]
10 }
```

The overall models for the DR circuits combines calls to these LuxR/LasR modules with calls to the eYFP /eCFP modules, but the latter uses more complex rate expressions that describe the complex inducible nature of the modified P_{Lux} promoters. As different DR circuits have different ribosome binding sites for LuxR and LasR expression, we use different values of a_R and a_S. Finally, we specify the initial conditions for C6 (species c6) and C12 (species c12) using parameters C6 and C12, which are set differently for each trace.

```

1 directive rates [
2   boundLuxR = [luxR]^2 * ((KR6*[c6])^nR + (KR12*[c12])^nR) / ((1.0 + KR6*[c6] + KR12*[c12])^nR);
3   boundLasR = [lasR]^2 * ((KS6*[c6])^nS + (KS12*[c12])^nS) / ((1.0 + KS6*[c6] + KS12*[c12])^nS);
4   P76 = (e76 + KGR_76*[boundLuxR] + KGS_76*[boundLasR]) / (1.0 + KGR_76*[boundLuxR] +
   KGS_76*[boundLasR]);
```

```

5     P81 = (e81 + KGR_81*[boundLuxR] + KGS_81*[boundLasR]) / (1.0 + KGR_81*[boundLuxR] +
6         KGS_81*[boundLasR]);
7 ]
7 device drPcat() = { LuxR(1.0,growth,capacity) | LasR(1.0,growth,capacity) |
    YFP(P81,aYFP,growth,capacity) | CFP(P76,aCFP,growth,capacity) }
8 device drRS100S32() = { LuxR(aRS100,growth,capacity) | LasR(aS32,growth,capacity) |
    YFP(P81,aYFP,growth,capacity) | CFP(P76,aCFP,growth,capacity) }
9 device drR33S32() = { LuxR(aR33,growth,capacity) | LasR(aS32,growth,capacity) |
    YFP(P81,aYFP,growth,capacity) | CFP(P76,aCFP,growth,capacity) }
10 device drR33S175() = { LuxR(aR33,growth,capacity) | LasR(aS175,growth,capacity) |
    YFP(P81,aYFP,growth,capacity) | CFP(P76,aCFP,growth,capacity) }

```

Characterization experiment

To characterize the LuxR and LasR signalling components, we used measurements of the response of four DR circuits from [3] to treatment with C6 and C12 over 3-fold dilutions. The maximum LuxR and LasR production rates were normalized to the values corresponding to the Pcat promoters, as done previously [3], thus setting the scale for unobserved concentrations of LuxR and LasR.

We used (uninformative) uniform priors on the previously uncharacterized parameters, and (informative) truncated Gaussian priors on f_{480} , f_{530} , d_{CFP} and d_{YFP} with mean and standard deviation taken from the marginal posteriors of the PRPR circuit characterization. These parameters are globally specified, with propagation of marginal posteriors as edges of the inference graph (see Listing 1). We also use uninformative priors on the B_k^{back} parameters (specified below as local parameters b530 and b480), without propagating their marginal posteriors from previous circuits.

As in the previous section, each system definition incorporates device invocations in combination with module calls for cell growth and autofluorescence.

```

1 // DR (Pcat-Pcat)
2 system dr_PcatPcat = {
3     directive simulation { final=36.0; points=250; plots=[[x]*([yfp]+[f530])+b530;
4         [x]*([cfp]+[f480])+b480]; plotcolours=["#FFDF00"; "#ADD8E6"] }
5     directive parameters [
6         r = 1, { interval=Real; distribution=Uniform(0.1,10); variation=Multiple };
7         K = 2, { interval=Real; distribution=Uniform(0.1,5); variation=Multiple };
8         tlag = 1, { interval=Real; distribution=Uniform(0,10); variation=Multiple };
9         rc=1e2, { interval=Log; distribution=Uniform(1e0,1e5); variation=Multiple };
10        b530=1e3, { interval=Real; distribution=Uniform(0.0,5e3); variation=Random };
11        b480=1e3, { interval=Real; distribution=Uniform(0.0,1e4); variation=Random };
12    ]
13    directive rates [growth = [grow]*r*(1 - [x] / K);capacity = rc]
14    directive crn { cells(growth,tlag) | autofluorescence(growth,capacity) }
15    | drPcat:device
16 }
17 // DR (R100-S32)
18 system dr_R100S32 = {
19     directive simulation { final=36.0; points=250; plots=[[x]*([yfp]+[f530])+b530;
20         [x]*([cfp]+[f480])+b480]; plotcolours=["#FFDF00"; "#ADD8E6"] }
21     directive parameters [
22         r = 1, { interval=Real; distribution=Uniform(0.1,10); variation=Multiple };
23         K = 2, { interval=Real; distribution=Uniform(0.1,5); variation=Multiple };
24         tlag = 1, { interval=Real; distribution=Uniform(0,10); variation=Multiple };
25         rc=1e2, { interval=Log; distribution=Uniform(1e0,1e5); variation=Multiple };
26         b530=1e3, { interval=Real; distribution=Uniform(0.0,5e3); variation=Random };
27         b480=1e3, { interval=Real; distribution=Uniform(0.0,1e4); variation=Random };
28    ]
29    directive rates [growth = [grow]*r*(1 - [x] / K);capacity = rc]

```

```

29     directive crn { cells(growth,tlag) | autofluorescence(growth,capacity) }
30     | drRS100S32:device
31 }
32
33 // DR (R33-S32)
34 system dr_R33S32 = {
35     directive simulation { final=36.0; points=250; plots=[[x]*([yfp]+[f530])+b530;
36         [x]*([cfp]+[f480])+b480]; plotcolours=["#FFDF00"; "#ADD8E6"] }
37     directive parameters [
38         r = 1, { interval=Real; distribution=Uniform(0.1,10); variation=Multiple };
39         K = 2, { interval=Real; distribution=Uniform(0.1,5); variation=Multiple };
40         tlag = 1, { interval=Real; distribution=Uniform(0,10); variation=Multiple };
41         rc=1e2, { interval=Log; distribution=Uniform(1e0,1e5); variation=Multiple };
42         b530=1e3, { interval=Real; distribution=Uniform(0.0,5e3); variation=Random };
43         b480=1e3, { interval=Real; distribution=Uniform(0.0,1e4); variation=Random };
44     ]
45     directive rates [growth = [grow]*r*(1 - [x] / K);capacity = rc]
46     directive crn { cells(growth,tlag) | autofluorescence(growth,capacity) }
47     | drR33S32:device
48 }
49 // DR (R33-S175)
50 system dr_R33S175 = {
51     directive simulation { final=36.0; points=250; plots=[[x]*([yfp]+[f530])+b530;
52         [x]*([cfp]+[f480])+b480]; plotcolours=["#FFDF00"; "#ADD8E6"] }
53     directive parameters [
54         r = 1, { interval=Real; distribution=Uniform(0.1,10); variation=Multiple };
55         K = 2, { interval=Real; distribution=Uniform(0.1,5); variation=Multiple };
56         tlag = 1, { interval=Real; distribution=Uniform(0,10); variation=Multiple };
57         rc=1e2, { interval=Log; distribution=Uniform(1e0,1e5); variation=Multiple };
58         b530=1e3, { interval=Real; distribution=Uniform(0.0,5e3); variation=Random };
59         b480=1e3, { interval=Real; distribution=Uniform(0.0,1e4); variation=Random };
60     ]
61     directive rates [growth = [grow]*r*(1 - [x] / K);capacity = rc]
62     directive crn { cells(growth,tlag) | autofluorescence(growth,capacity) }
63     | drR33S175:device
64 }

```

Characterization results

In the subsequent figures we first show model-data comparisons for the TargetSwitch hypothesis applied using direct (Fig. S9) and ratiometric characterization (Figs. S10 & S11). Next, we show the marginal posterior distributions for each parameter (Figs. S12 & S13).

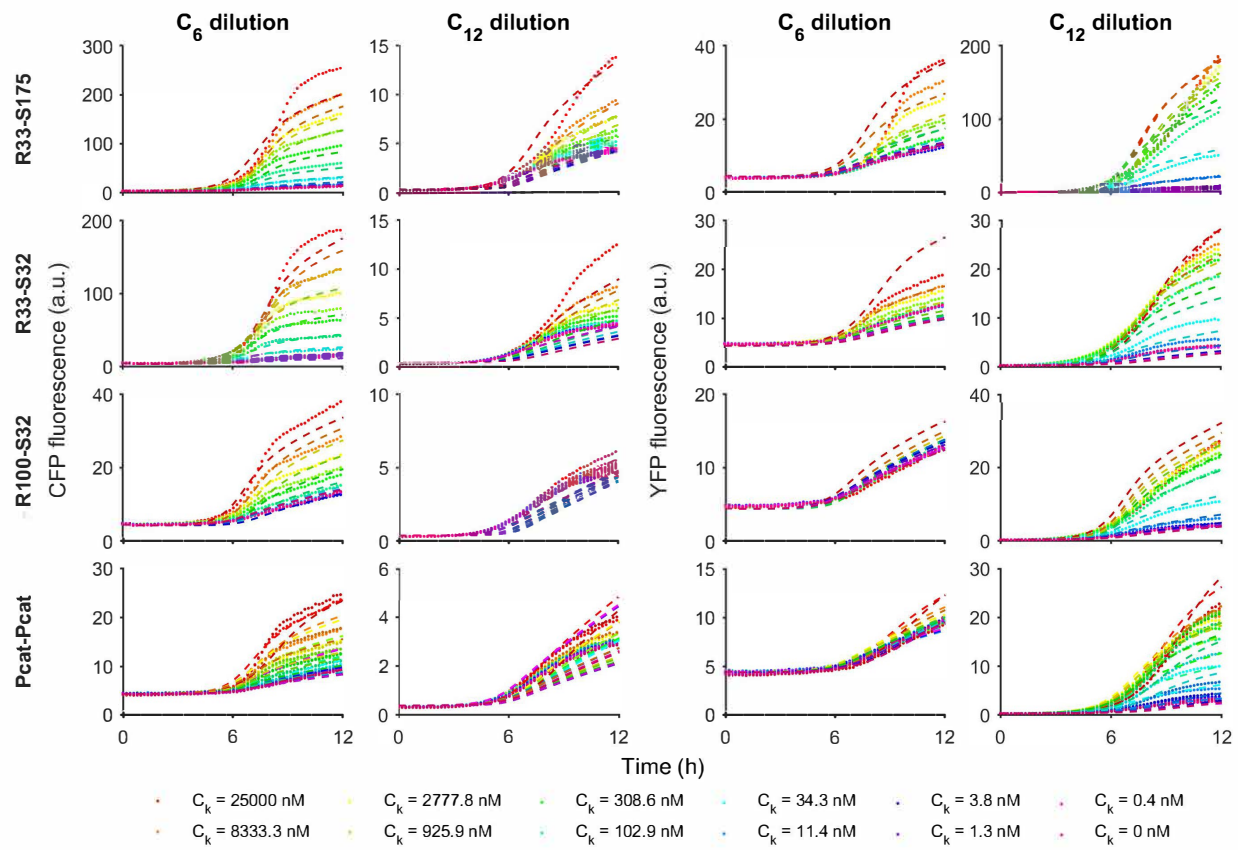


Figure S9: Model-data comparison for Receivers using direct dynamic characterization with the TargetSwitch hypothesis.

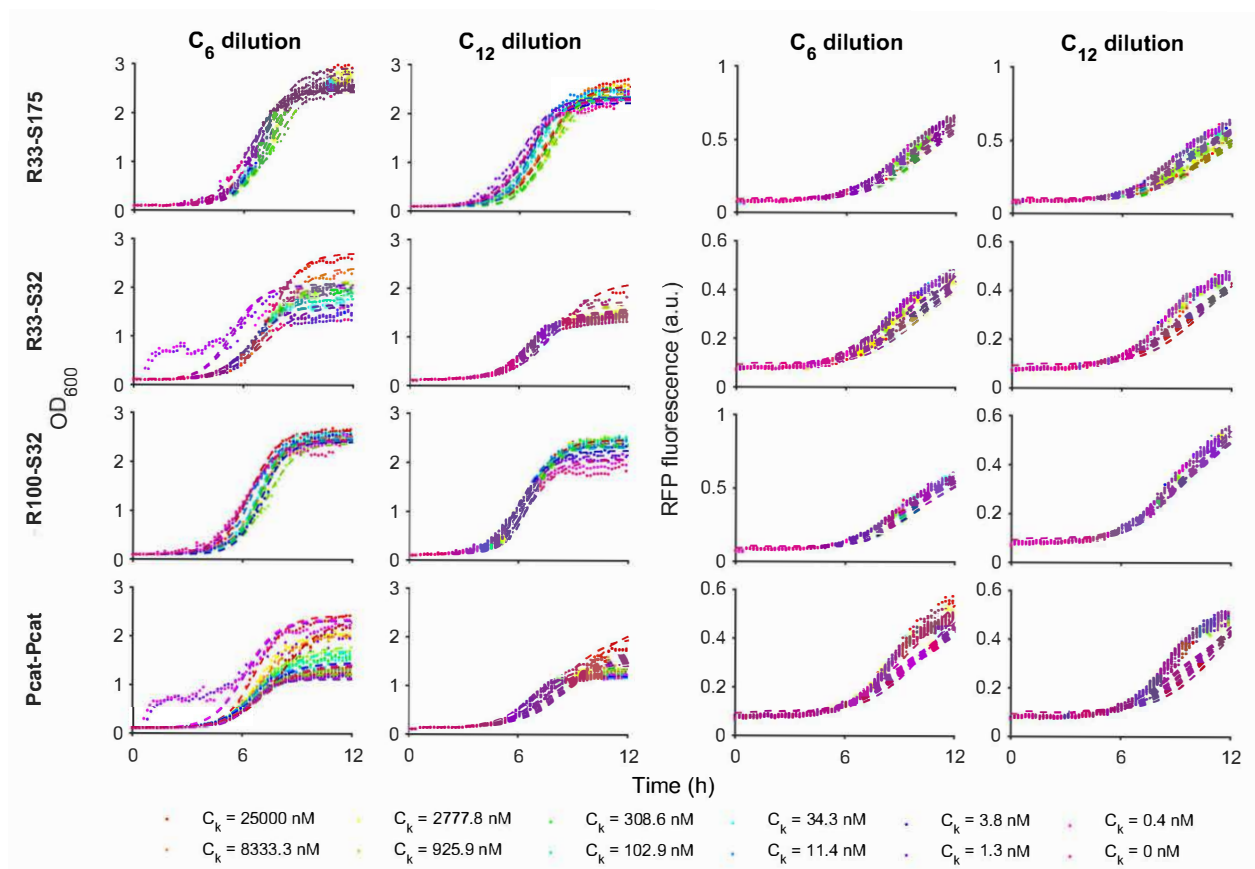


Figure S10: Model-data comparison for Receivers using ratiometric dynamic characterization with the TargetSwitch hypothesis (Growth and Control phases).

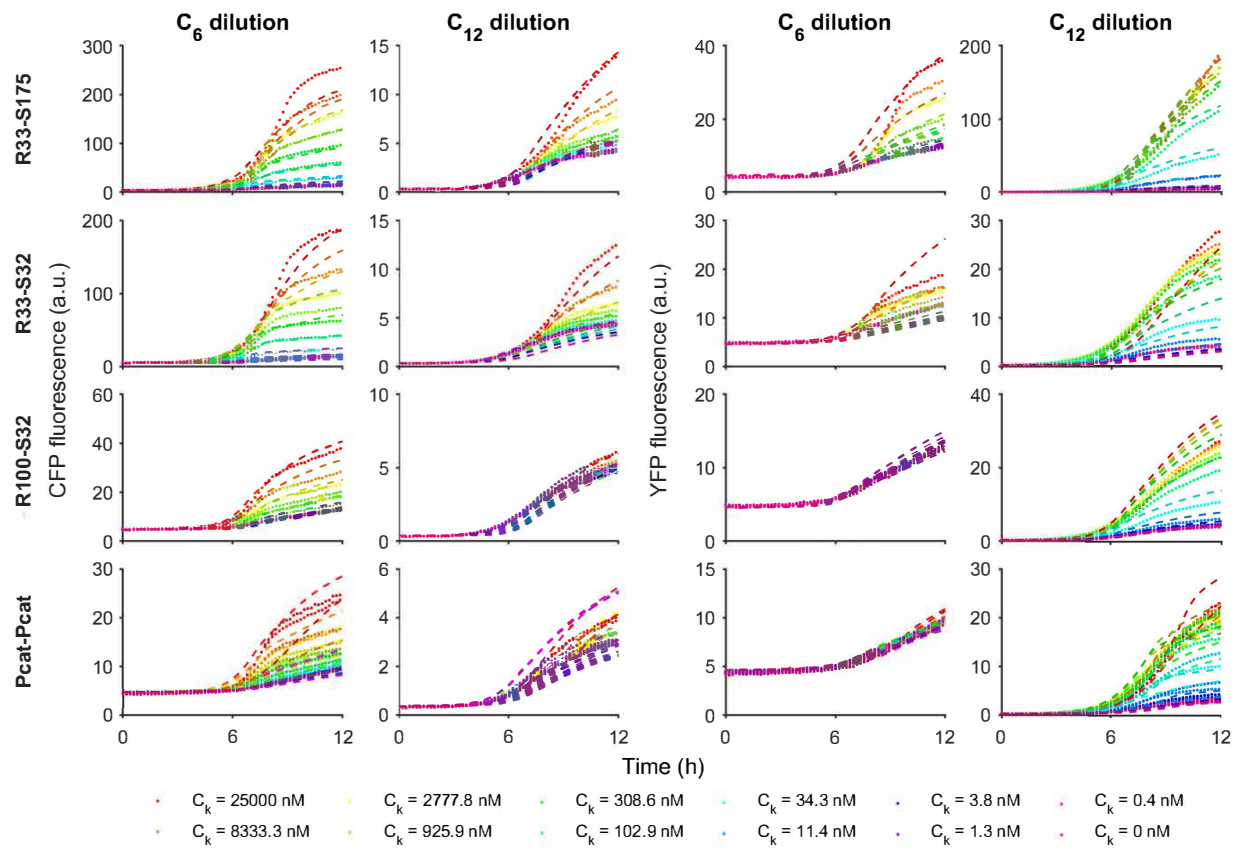


Figure S11: Model-data comparison for Receivers using ratiometric dynamic characterization with the TargetSwitch hypothesis.

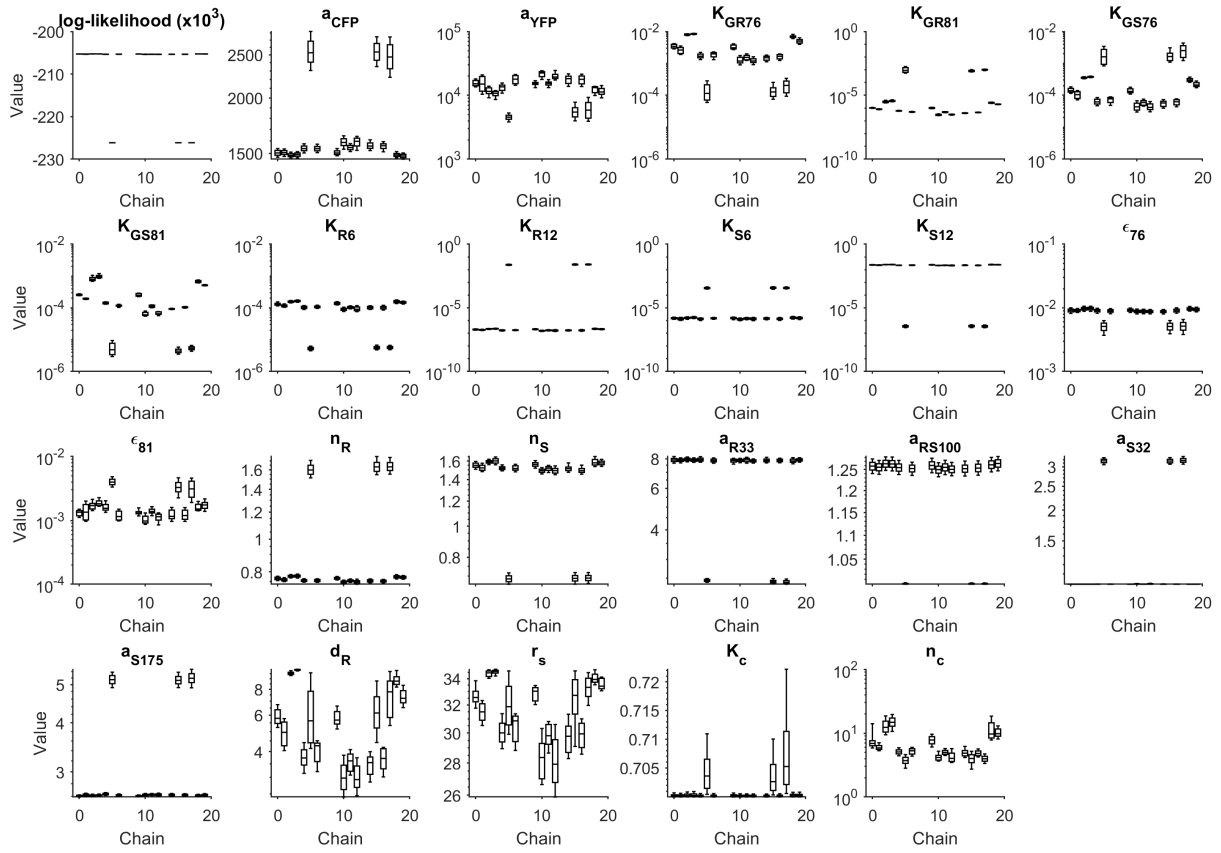


Figure S12: Marginal parameter posterior distributions for the DR circuit with TargetSwitch using the direct method. Inference of circuit parameters using the direct (non-ratiometric) method, which corresponds to assuming that $r_c = 1$ for all time-series traces.

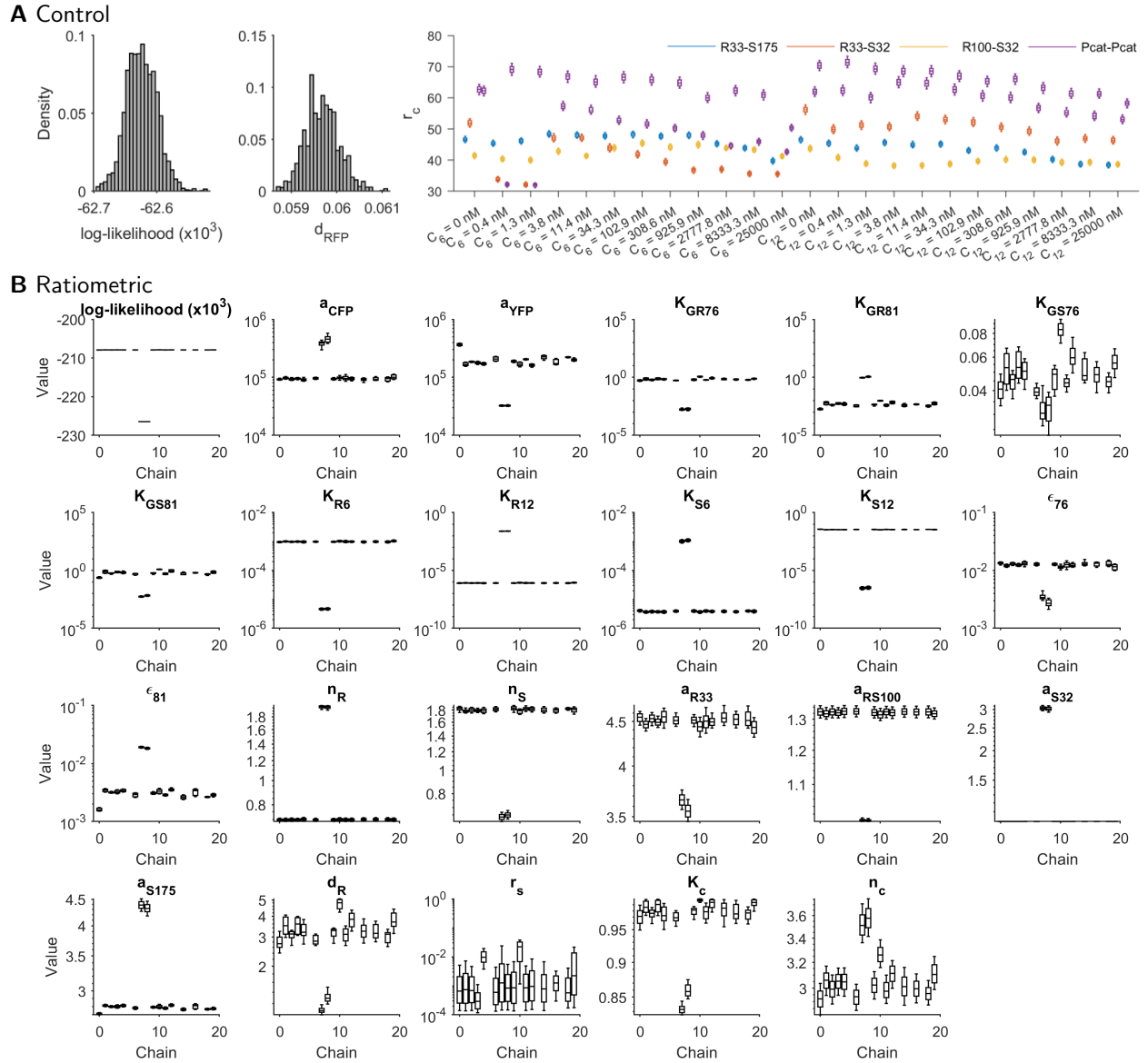


Figure S13: Marginal parameter posterior distributions for the DR circuit with TargetSwitch using the ratiometric method. A. The control phase identifies values for r_c for each time-series, to be used in ratiometric characterization. **B.** Inference of circuit parameters using the ratiometric method, using the values of r_c in B.

S2.4 AHL senders (Relays)

To characterize the dynamics of AHL senders, we constructed two *relay* signalling devices, each perceiving a first signal that acts as an inducer for a second signal. The first relay device responds to C6 via binding of constitutively expressed LuxR and activation of the engineered PLux76 promoter, then synthesizes the C12-producing LasI enzyme and eCFP. C12 is then detected via binding of constitutively expressed LasR and activation of the engineered PLas81 promoter, which synthesizes eYFP. Accordingly, we can monitor the promoter activity of both stages of the relay signals. The second device performs receive-send-receive in the other order, sensing C12 via PLas81, which synthesizes the C6-producing LuxI enzyme (and eYFP), with C6 then detected via PLux76-eCFP. Both relay circuits embed the double receiver module, along with an HSL sender for C6 or for C12 (Fig. S14). As such, the parameter posterior distributions learned during characterization of the double receiver module are relevant prior distributions for these circuits.

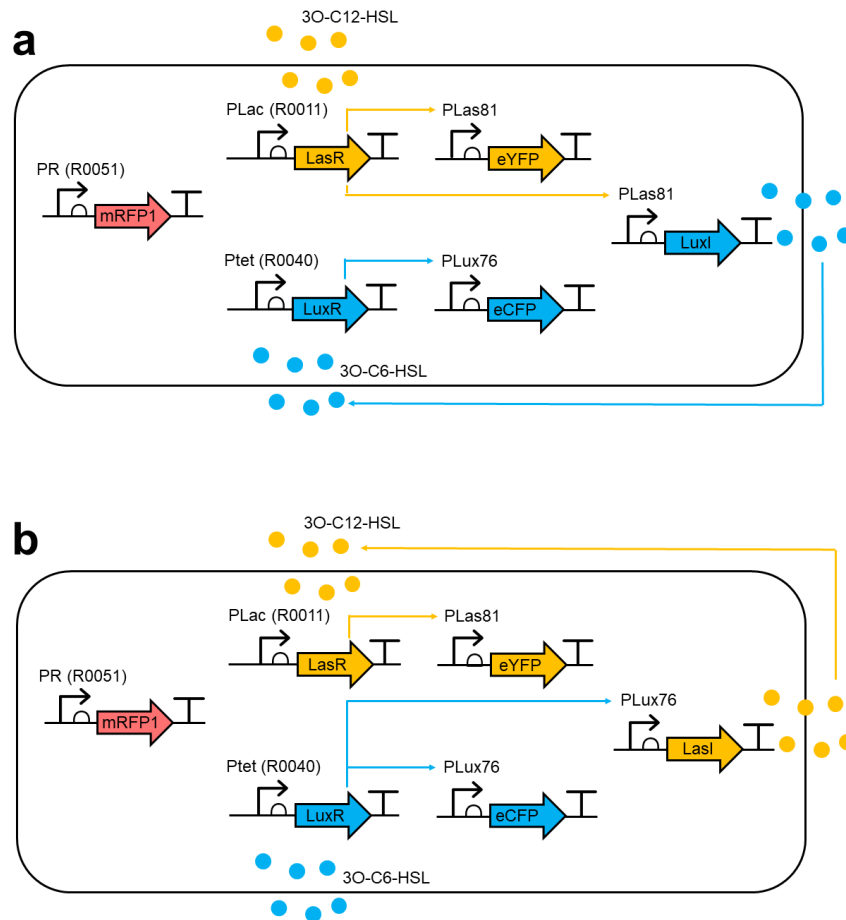


Figure S14: Relay circuit network diagrams. A. The PLas81-LuxI relay device, with double reporter. B. The PLux76-LasI device, with double reporter.

Model definition

The models for the relay circuits are modular: the double receiver model from Section S2.3, is extended by equations for *luxI* and *lasI*, and additional terms for C_6 and C_{12} synthesis. Building on the approach above, we can write down an equation for the intracellular production of LuxI or LasI. Each then synthesizes C_6 and C_{12} respectively, which we model as a linear function of $[luxI]$ or $[lasI]$. In the models described above, it was assumed that transport between the intracellular and extracellular compartments was fast. As there was no *de novo* synthesis of HSL, and often a large extracellular excess, the system dynamics would

unlikely be critically sensitive to this approximation, as any lag could be accounted for by adjustments in the other parameters. However, in the relay circuits, where HSLs are being produced, the transport between intracellular and extracellular compartments must be considered more carefully. For the C6-LasI-C12 relay, the equations for the mass of each molecule in the intracellular (denoted by subscript i) and extracellular (denoted by subscript e) compartments is given by

$$\frac{d(V_i \cdot [\text{lasI}])}{dt} = V_i \cdot h \left(\frac{V_i}{V_{\text{tot}}} \right) \cdot \rho_L \cdot f_{76}([C_6], [C_{12}], [\text{luxR}], [\text{lasR}]) - V_i \cdot d_L [\text{lasI}] \quad (\text{S20a})$$

$$\frac{d(V_i \cdot [C_{12}]_i)}{dt} = V_i \cdot k_{C12} \cdot [\text{lasI}] + \eta_{12} ([C_{12}]_e - [C_{12}]_i) \quad (\text{S20b})$$

$$\frac{d(V_e \cdot [C_{12}]_e)}{dt} = \eta_{12} ([C_{12}]_i - [C_{12}]_e) \quad (\text{S20c})$$

where ρ_L is the relative production rate of lasI (relative to eCFP production; see above), and k_{C12} is the rate of C12 synthesis by lasI. Here, V_i and V_e are the volumes of intracellular and extracellular compartments respectively. Accordingly, cell density c is simply the ratio of V_i to $V_i + V_e =: V_{\text{tot}}$.

To arrive at a set of equations for the derivatives of the concentrations of each molecule (in each compartment), we expand the left-hand sides using the chain rule. Then, defining $\gamma := \frac{1}{V_i} \frac{dV_i}{dt}$ as the specific growth rate, or *dilution* factor, assuming that $V_e = V_{\text{tot}} - V_i$, and rescaling $[\text{lasI}]$ according to $[\text{lasI}] = \frac{L}{\rho_L}$ we obtain

$$\frac{dL}{dt} = h \left(\frac{V_i}{V_{\text{tot}}} \right) \cdot f_{76}([C_6], [C_{12}], [\text{luxR}], [\text{lasR}]) - (d_L + \gamma)L \quad (\text{S21a})$$

$$\frac{d[C_{12}]_i}{dt} = k'_{C12} \cdot L + \frac{\eta_{12}}{V_i} ([C_{12}]_e - [C_{12}]_i) - \gamma [C_{12}]_i \quad (\text{S21b})$$

$$\frac{d[C_{12}]_e}{dt} = \frac{\eta_{12}}{V_{\text{tot}} - V_i} ([C_{12}]_i - [C_{12}]_e) + \frac{\gamma V_i}{V_{\text{tot}} - V_i} \quad (\text{S21c})$$

where $k'_{C12} = \frac{k_{C12}}{\rho_L}$.

As we had no reliable estimate of HSL transport rates *a priori*, we started by using the model that combines (S21) with (S19). However, we also considered the assumption that HSL transport is fast, resulting in the relations $[C_k]_e = [C_k]_i = [C_k]$ for $k = 6, 12$. By summing equations (S20b) and (S20c), and using an equivalent rescaling for $[\text{lasI}]$ as before, we obtain

$$\frac{d(V_{\text{tot}} \cdot [C_{12}])}{dt} = \frac{d(V_i \cdot [C_{12}]_i)}{dt} + \frac{d(V_e \cdot [C_{12}]_e)}{dt} = V_i \cdot k_{C12} \cdot L$$

which when rearranged and gives an alternative to model (S21) as

$$\frac{dL}{dt} = h(c) \cdot f_{76}([C_6], [C_{12}], [\text{luxR}], [\text{lasR}]) - (d_L + \gamma)L \quad (\text{S22a})$$

$$\frac{d[C_{12}]}{dt} = k'_{C12} \cdot c \cdot L \quad (\text{S22b})$$

with k'_{C12} and L as defined above.

Saturation of HSL substrate usage. If the luxI or lasI enzymes are expressed very highly, it might be that substrate becomes the limiting factor for HSL synthesis (as opposed to enzyme). In which case, a saturating production term should be used, which is parametrized by a new parameter K_L , the concentration of luxI/lasI at which HSL production is half-maximal. We can define this function as

$$f(L) = k'_{C12} \cdot \frac{L}{L + K_L} \quad (\text{S23})$$

where k'_{C12} is the rescaled (maximal) per-enzyme rate of HSL synthesis from lasI, as above.

Finally, we note that the equations above can be trivially concatenated with the equations of the double receiver device described in the previous section to produce a full model of each relay device.

Implementation with GEC/CRN language

We define modules for LuxI and LasI enzymes, which includes their modelled enzymatic synthesis of C6 and C12. As before, we use a rate expression argument to arbitrarily assign a promoter transfer function to the production rates of each enzyme. However, since LuxI and LasI are never observed, their maximal production rates can be *divided out*, as explained above, and without loss of generality set to a value 1.

```
1 module LuxI(P,growth,capacity) = {
2   ->[[capacity]*[P]] luxI |
3   luxI ->{dLuxI} |
4   luxI ->[[growth]*[luxI]] |
5   ->[kC6*[capacity]*[x]*[luxI]/(1+[luxI]/Klux)] c6
6 }
7 module LasI(P,growth,capacity) = {
8   ->[[capacity]*[P]] lasI |
9   lasI ->{dLasI} |
10  lasI ->[[growth]*[lasI]] |
11  ->[kC12*[capacity]*[x]*[lasI]/(1+[lasI]/Klas)] c12
12 }
13
14 device drR33S175() = { LuxR(aR33,growth,capacity) | LasR(aS175,growth,capacity) |
15   YFP(P81,aYFP,growth,capacity) | CFP(P76,aCFP,growth,capacity) }
16 device relayP76LasI() = { LasI(P76,growth,capacity) }
17 device relayP81LuxI() = { LuxI(P81,growth,capacity) }
```

Characterization experiment

To characterize the Relay devices, we measured each in response to C6 and C12 treatments. We used (uninformative) uniform priors on the previously uncharacterized parameters (k_{C6} , k_{C12} , K_{lux} , K_{las} , d_{luxI} and d_{lasI}), and (informative) truncated Gaussian priors on all remaining parameters, with mean and standard deviation taken from the marginal posteriors of the DR circuits characterization. We also use uninformative priors on the background fluorescence parameters (specified below as local parameters b530 and b480), without propagating their marginal posteriors from previous circuits.

To instantiate the relay circuits, we use device definitions as above, this time taking advantage of device modularity.

```
1 system relay_P76LasI = {
2   directive simulation { final=36.0; points=250; plots=[[x]*([yfp]+[f530])+b530;
3     [x]*([cfp]+[f480])+b480]; plotcolours=["#FFDF00"; "#ADD8E6"] }
4   directive parameters [
5     r = 1, { interval=Real; distribution=Uniform(0.1,10); variation=Multiple };
6     K = 2, { interval=Real; distribution=Uniform(0.1,5); variation=Multiple };
7     tlag = 1, { interval=Real; distribution=Uniform(0,10); variation=Multiple };
8     rc=1e2, { interval=Log; distribution=Uniform(1e0,1e5); variation=Multiple };
9     b530=1e3, { interval=Real; distribution=Uniform(0.0,5e3); variation=Random };
10    b480=1e3, { interval=Real; distribution=Uniform(0.0,1e4); variation=Random };
11  ]
12  directive rates [growth = [grow]*r*(1 - [x] / K);capacity = rc]
13  directive crn { cells(growth,tlag) | autofluorescence(growth,capacity) }
14  | drR33S175:device
15  | relayP76LasI:device
16 }
17 system relay_P81LuxI = {
18   directive simulation { final=36.0; points=250; plots=[[x]*([yfp]+[f530])+b530;
19     [x]*([cfp]+[f480])+b480]; plotcolours=["#FFDF00"; "#ADD8E6"] }
20   directive parameters [
21     r = 1, { interval=Real; distribution=Uniform(0.1,10); variation=Multiple };
```

```

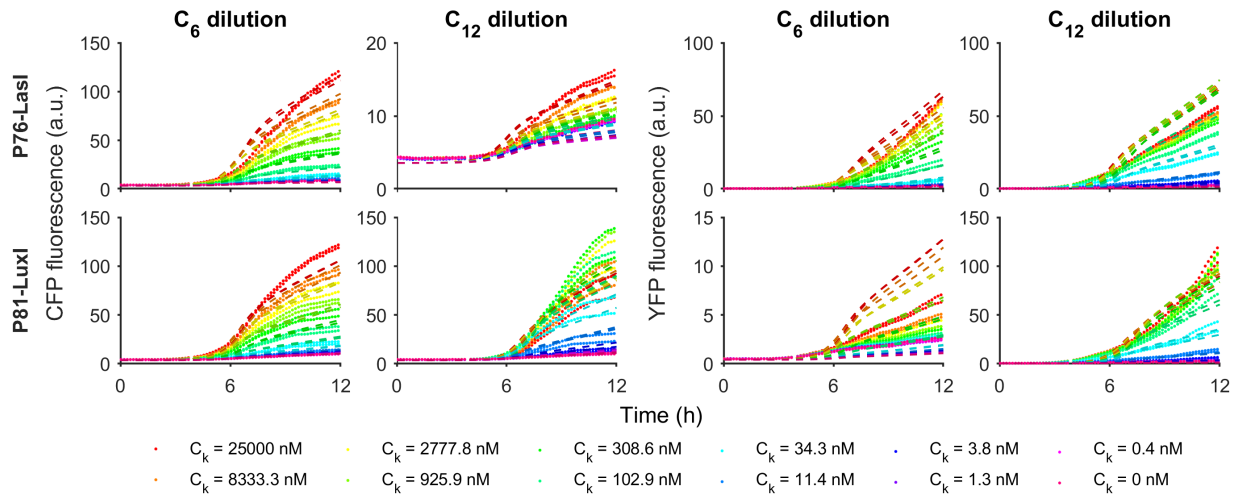
21     K = 2, { interval=Real; distribution=Uniform(0.1,5); variation=Multiple };
22     tlag = 1, { interval=Real; distribution=Uniform(0,10); variation=Multiple };
23     rc=1e2, { interval=Log; distribution=Uniform(1e0,1e5); variation=Multiple };
24     b530=1e3, { interval=Real; distribution=Uniform(0.0,5e3); variation=Random };
25     b480=1e3, { interval=Real; distribution=Uniform(0.0,1e4); variation=Random };
26 ]
27 directive rates [growth = [grow]*r*(1 - [x] / K);capacity = rc]
28 directive crn { cells(growth,tlag) | autofluorescence(growth,capacity) }
29 | drR33S175:device
30 | relayP81LuxI:device
31 }

```

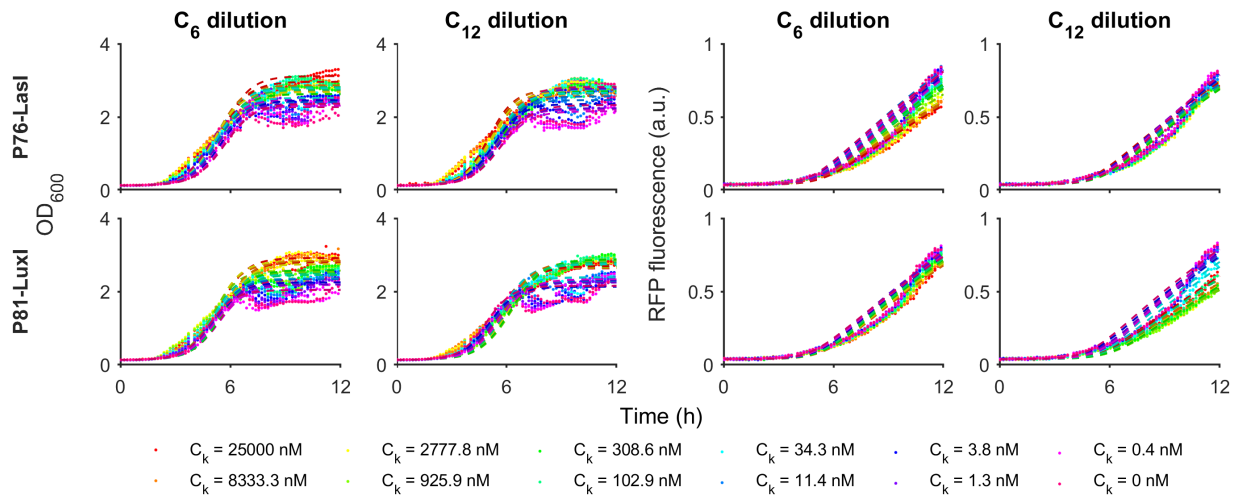
Characterization results

In the subsequent figures we first show model-data comparisons for the TargetSwitch hypothesis applied using direct (Fig. S15A) and ratiometric characterization (Fig. S15B,C). Next, we show the marginal posterior distributions for each parameter (Fig. S16).

A Direct



B Control



C Ratiometric

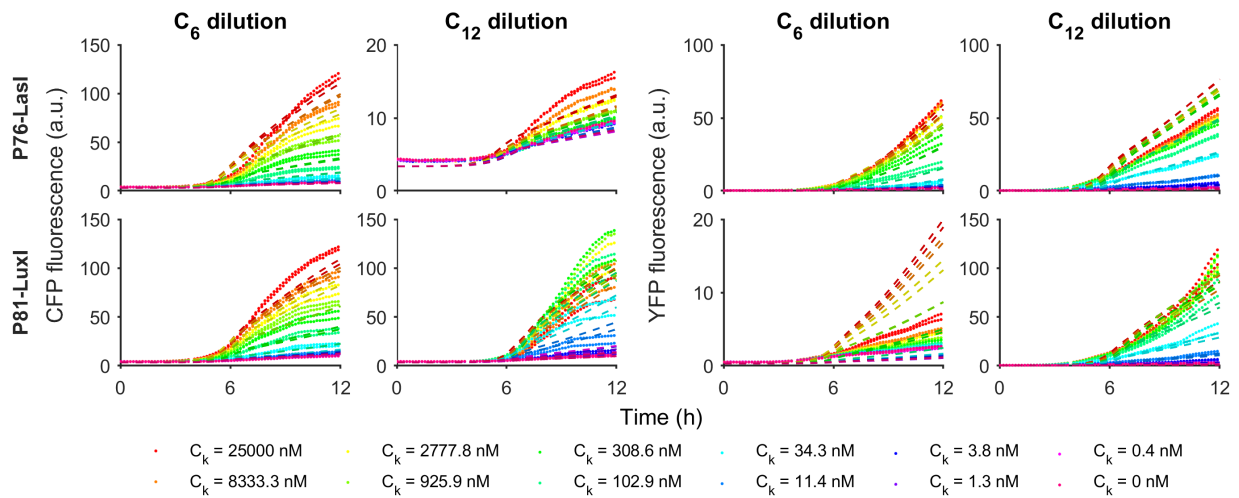


Figure S15: Model-data comparison for the Relays circuit with TargetSwitch. Measurements of the Relays circuit are compared against simulations of the maximum likelihood parameter set from the TargetGrowth hypothesis.

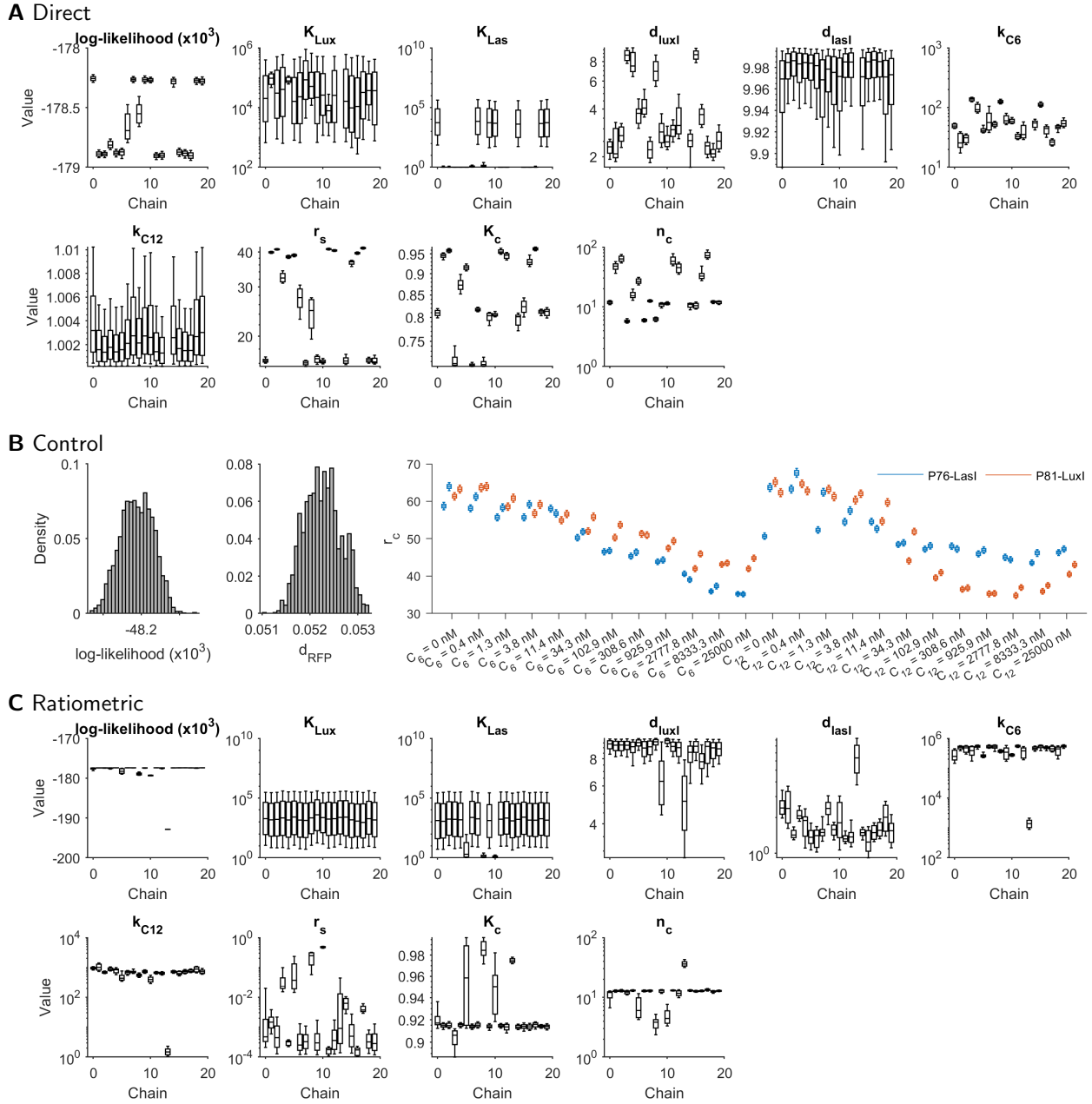


Figure S16: Marginal parameter posterior distributions for Relays with TargetSwitch hypothesis. **A.** Inference of circuit parameters using the direct (non-ratiometric) method, which corresponds to assuming that $r_c = 1$ for all time-series traces. **B.** The control phase identifies values for r_c for each time-series, to be used in ratiometric characterization. **C.** Inference of circuit parameters using the ratiometric method, using the values of r_c in B.

S2.5 Inducible expression (PBAD)

The arabinose-PBAD system is commonly used to control expression in synthetic gene circuits. The PBAD promoter is part of the arabinose operon, which also involves the araC protein. When arabinose is added to cell cultures at different concentrations, it increases expression of a downstream transcript. In this study, we have used PBAD to control AHL lactonase expression (see Section S2.6 for details).

To characterize the relationship between PBAD and arabinose in vivo, we constructed the Inducer circuit, which has the coding sequence for eYFP downstream of PBAD, and measured its response to varying concentrations of arabinose.

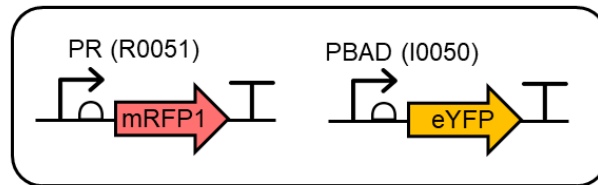


Figure S17: Design of Inducer circuit.

Characterization experiment

We measured the Inducer circuit in response to varying concentrations of the arabinose inducer. We used (uninformative) uniform priors on the previously uncharacterized parameters, and (informative) truncated Gaussian priors on a_{480} and a_{530} with mean and standard deviation taken from the marginal posteriors of the Constitutive circuit characterization. We also use uninformative priors on the background fluorescence parameters, without propagating their marginal posteriors from previous circuits.

Implementation with GEC/CRN language

As the module for describing eYFP expression has already been defined, it can be used directly to describe PBAD induction. All that is required is to define a rate expression for the transfer function that describes PBAD activity in response to varying concentrations of arabinose, and define a new parameter that quantifies maximal YFP production in the context of a PBAD promoter (with B0034 ribosome binding site). Accordingly, the Inducer circuit is described by

```
1 directive rates [  
2   PBAD = (Ara^nA+eA*KAra^nA)/(Ara^nA+KAra^nA);  
3 ]  
4  
5 device pBADYFP() = { YFP(PBAD,aYFP,growth,capacity) }  
6  
7 system PBADYFP = { target with  
8   directive simulation { final=36.0; points=250; plots=[[x]*([yfp]+[f530])+b530];  
9     plotcolours=["#FFDF00"] }  
10  directive parameters [  
11    r = 1, { interval=Real; distribution=Uniform(0.1,10); variation=Multiple };  
12    K = 2, { interval=Real; distribution=Uniform(0.1,5); variation=Multiple };  
13    tlag = 1, { interval=Real; distribution=Uniform(0,10); variation=Multiple };  
14    rc=1e2, { interval=Log; distribution=Uniform(1e0,1e5); variation=Multiple };  
15    aYFP=1.0, { interval=Log; distribution=Uniform(1e0,1e5); variation=Random };  
16    b530=1e3, { interval=Real; distribution=Uniform(0.0,5e3); variation=Random };  
17  ]  
18  directive rates [growth = [grow]*r*(1 - [x] / K);capacity = rc]  
19  directive crn { cells(growth,tlag) | autofluorescence(growth,capacity) }  
20  pBadYFP:device  
21 }
```


Characterization results

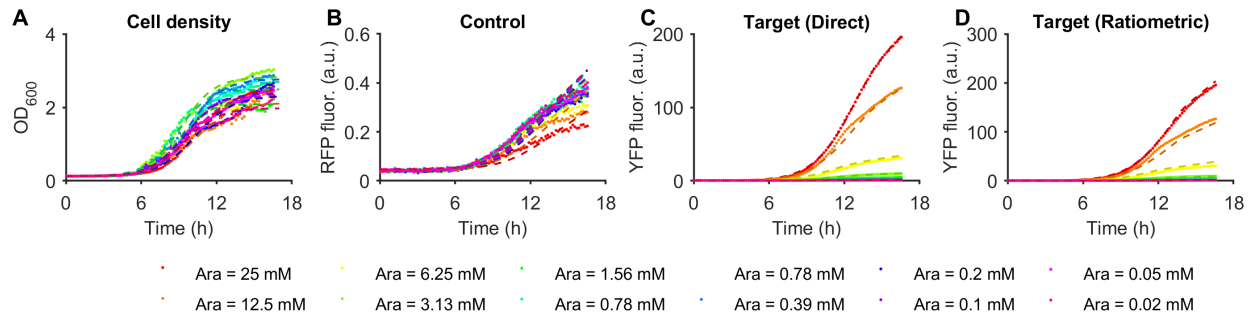


Figure S18: Model-data comparison for the Inducer circuit with TargetSwitch hypothesis. Measurements of the PBADYFP circuit are compared against simulations of the maximum likelihood parameter set from applying ratiometric dynamic characterization with the TargetSwitch hypothesis.

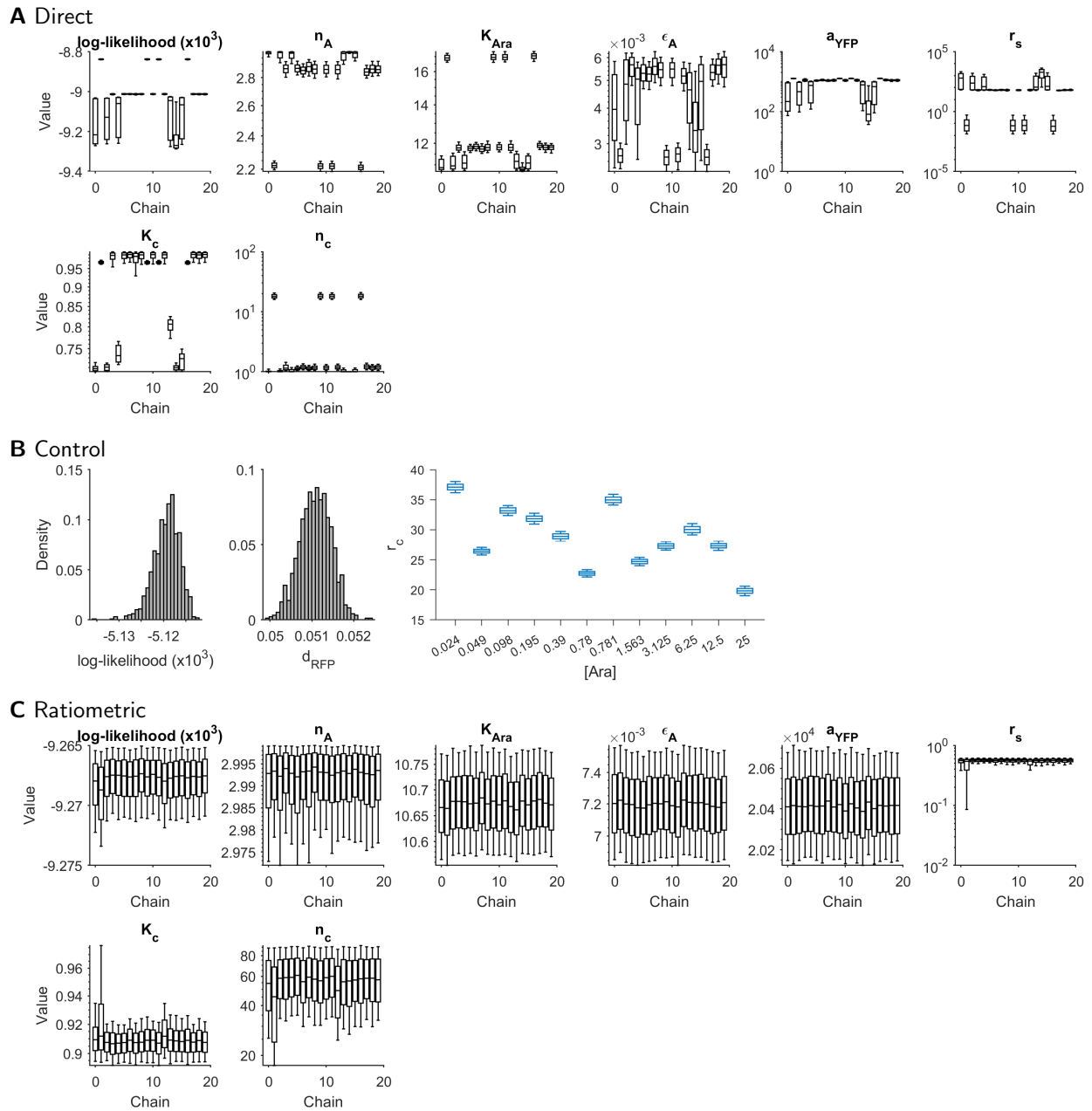


Figure S19: Marginal parameter posterior distributions for the Inducer circuit with TargetSwitch hypothesis. A. Inference of circuit parameters using the direct (non-ratiometric) method, which corresponds to assuming that $r_c = 1$ for all time-series traces. **B.** The control phase identifies values for r_c for each time-series, to be used in ratiometric characterization. **C.** Inference of circuit parameters using the ratiometric method, using the values of r_c in B.

S2.6 HSL lactonase (AiiA)

AHL molecules can be degraded by AHL lactonase enzymes. The most commonly used lactonase in synthetic biology applications is AiiA [5, 6], which originates from *Bacillus Thuringensis*. AiiA is mostly non-specific; catalytic activity has been measured against a large variety of AHLs with varying length carbon chains [7].

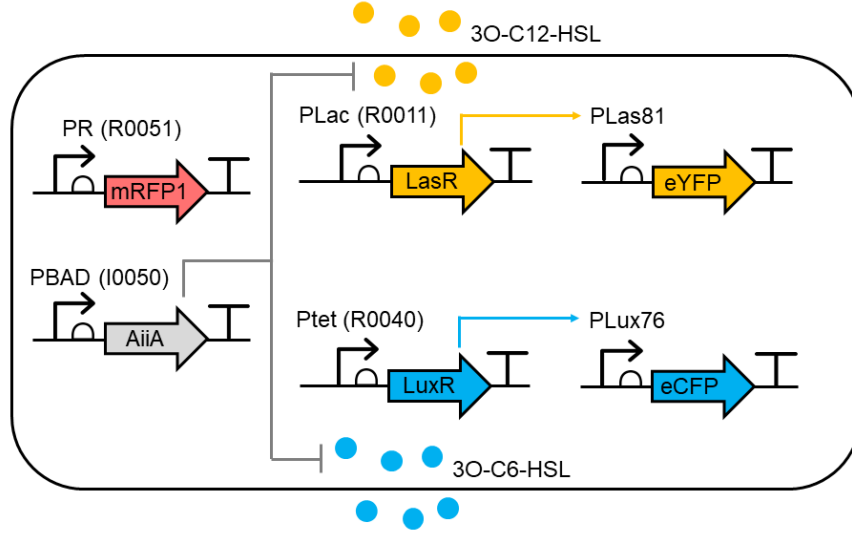
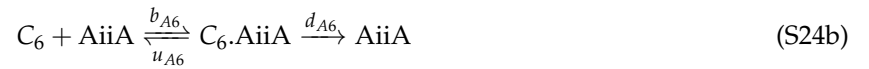


Figure S20: Network diagram for the Degradier circuit.

To characterize the AiiA lactonase activity in a synthetic gene circuit, we constructed a PBAD-AiiA plasmid, and combined this with the R33-S175 plasmid to define an arabinose-inducible Degradier circuit (Fig. S20).

It is fairly straightforward to write down a few reactions describing the production, degradation and catalytic activity of AiiA. Assuming constitutive production, we propose:



As AHLs may translocate between cells and the extracellular medium, and AiiA is only expressed inside cells, we must carefully consider the volume and concentration of these molecules over time, as before.

Translating the above reactions to ODEs, we obtain

$$\frac{d(V_i \cdot [A])}{dt} = V_i \cdot a_A \cdot f_{\text{Pbad}}(\text{Ara}) + V_i \cdot (u_{A6} + d_{A6})[A \cdot C_6] + V_i \cdot (u_{A12} + d_{A12})[A \cdot C_{12}] \dots \quad (\text{S25a})$$

$$- V_i \cdot (d_A + b_{A6}[C_6]_i + b_{A12}[C_{12}]_i)[A] \quad (\text{S25b})$$

$$\frac{d(V_i \cdot [C_6]_i)}{dt} = V_i \cdot u_{A6} \cdot [A \cdot C_6] + \eta_6 ([C_6]_e - [C_6]_i) - V_i \cdot (d_C + b_{A6}[A])[C_6]_i \quad (\text{S25c})$$

$$\frac{d(V_i \cdot [C_{12}]_i)}{dt} = V_i \cdot u_{A12} \cdot [A \cdot C_{12}] + \eta_{12} ([C_{12}]_e - [C_{12}]_i) - V_i \cdot (d_C + b_{A12}[A])[C_{12}]_i \quad (\text{S25d})$$

$$\frac{d(V_i \cdot [A \cdot C_6])}{dt} = V_i \cdot b_{A6}[A][C_6]_i - V_i \cdot (u_{A6} + d_{A6})[A \cdot C_6] \quad (\text{S25e})$$

$$\frac{d(V_i \cdot [A \cdot C_{12}])}{dt} = V_i \cdot b_{A6}[A][C_{12}]_i - V_i \cdot (u_{A12} + d_{A12})[A \cdot C_{12}] \quad (\text{S25f})$$

$$\frac{d(V_e \cdot [C_6]_e)}{dt} = \eta_6 ([C_6]_i - [C_6]_e) \quad (\text{S25g})$$

$$\frac{d(V_e \cdot [C_{12}]_e)}{dt} = \eta_{12} ([C_{12}]_i - [C_{12}]_e) \quad (\text{S25h})$$

We can apply an equilibrium assumption to the AiiA-HSL intermediate by equating (S25e) and (S25f) to zero. This gives

$$[A \cdot C_j] = \frac{b_{Aj}}{\gamma + u_{Aj} + d_{Aj}} [A][C_j] \approx \frac{b_{Aj}}{u_{Aj} + d_{Aj}} [A][C_j] \quad (\text{S26})$$

where the approximation to suppress γ is due to the catalytic activity of AiiA being significantly faster than the dilution rate. Therefore, depending on the concentrations $[C_6]$ and $[C_{12}]$, AiiA is bound according to the conservation equation

$$[A_{\text{Tot}}] = [A] + [A \cdot C_6] + [A \cdot C_{12}] = [A] \cdot (1 + K_{A6}[C_6] + K_{A12}[C_{12}]) \quad (\text{S27})$$

where $K_{Aj} = \frac{b_{Aj}}{u_{Aj} + d_{Aj}}$. By cancelling the binding and unbinding terms with AiiA, we are left with the simpler set of equations

$$\frac{d(V_i \cdot [A_{\text{Tot}}])}{dt} = V_i \cdot a_A \cdot f_{\text{Pbad}}(\text{Ara}) - V_i \cdot d_A \cdot \frac{[A_{\text{Tot}}]}{1 + K_{A6}[C_6] + K_{A12}[C_{12}]} \quad (\text{S28a})$$

$$\frac{d(V_i \cdot [C_6]_i)}{dt} = \eta_6 ([C_6]_e - [C_6]_i) - V_i \cdot d_{A6} \cdot \frac{[A_{\text{Tot}}][C_6]_i}{1 + K_{A6}[C_6]_i + K_{A12}[C_{12}]_i} - V_i \cdot d_C \cdot [C_j] \quad (\text{S28b})$$

$$\frac{d(V_i \cdot [C_{12}]_i)}{dt} = \eta_{12} ([C_{12}]_e - [C_{12}]_i) - V_i \cdot d_{A12} \cdot \frac{[A_{\text{Tot}}][C_{12}]_i}{1 + K_{A6}[C_6]_i + K_{A12}[C_{12}]_i} - V_i \cdot d_C \cdot [C_j] \quad (\text{S28c})$$

$$\frac{d(V_e \cdot [C_6]_e)}{dt} = \eta_6 ([C_6]_i - [C_6]_e) \quad (\text{S28d})$$

$$\frac{d(V_e \cdot [C_{12}]_e)}{dt} = \eta_{12} ([C_{12}]_i - [C_6]_e) \quad (\text{S28e})$$

As before, we seek a system of equations for the rates of change of the molecular concentrations, but distinguish between whether we assume that transport is fast enough to remove from the model or not. We additionally augment each equation system with the double receiver module.

Slow transport model

We start by expanding the derivatives on the left-hand sides, then defining $\gamma := \frac{1}{V_i} \frac{dV_i}{dt}$ as the specific growth rate, or *dilution* factor. Therefore, we obtain

$$\frac{d[A]}{dt} = a_A \cdot f_{\text{Pbad}}(\text{Ara}) - (d_A + \gamma) \cdot [A] \quad (\text{S29a})$$

$$\frac{d[C_6]_i}{dt} = \frac{1}{V_i} \cdot \eta_6 ([C_6]_e - [C_6]_i) - d_{A6} \cdot \frac{[A][C_6]_i}{1 + K_{A6}[C_6]_i + K_{A12}[C_{12}]_i} - (d_C + \gamma) \cdot [C_j] \quad (\text{S29b})$$

$$\frac{d[C_{12}]_i}{dt} = \frac{1}{V_i} \cdot \eta_{12} ([C_{12}]_e - [C_{12}]_i) - d_{A12} \cdot \frac{[A][C_{12}]_i}{1 + K_{A6}[C_6]_i + K_{A12}[C_{12}]_i} - (d_C + \gamma) \cdot [C_j] \quad (\text{S29c})$$

$$\frac{d[C_6]_e}{dt} = \frac{1}{V_e} \cdot \eta_6 ([C_6]_i - [C_6]_e) - \frac{1}{V_e} \cdot \frac{dV_e}{dt} \quad (\text{S29d})$$

$$\frac{d[C_{12}]_e}{dt} = \frac{1}{V_e} \cdot \eta_{12} ([C_{12}]_i - [C_6]_e) - \frac{1}{V_e} \cdot \frac{dV_e}{dt} \quad (\text{S29e})$$

Two assumptions could be applied to V_e : (1) V_e is constant, or (2) $V_e = V_{\text{tot}} - V_i$, where V_{tot} is a fixed total volume.

Fast transport model

If we assume that HSL transport is infinitely fast, then this results in the relations $[C_k]_e = [C_k]_i = [C_k]$ for $k = 6, 12$. However, we must be careful to maintain conservation of mass with respect to AiiA-mediated degradation. That is, we must scale the stoichiometric loss of HSL by the ratio of the extracellular and intracellular volumes. To see this, we write out equations for the new variables $[C_k]$ in terms of its constituent compartments.

$$\frac{d(V_i \cdot [A])}{dt} = V_i \cdot a_A \cdot f_{\text{Pbad}}(\text{Ara}) - V_i \cdot d_A \cdot [A] \quad (\text{S30a})$$

$$\frac{d(V \cdot [C_6])}{dt} = \frac{d(V_i \cdot [C_6]_i)}{dt} + \frac{d(V_e \cdot [C_6]_e)}{dt} = -V_i \cdot d_{A6} \cdot \frac{[A][C_6]}{1 + K_{A6}[C_6] + K_{A12}[C_{12}]} - V_i \cdot d_C \cdot [C_6] \quad (\text{S30b})$$

$$\frac{d(V \cdot [C_{12}])}{dt} = \frac{d(V_i \cdot [C_{12}]_i)}{dt} + \frac{d(V_e \cdot [C_{12}]_e)}{dt} = -V_i \cdot d_{A12} \cdot \frac{[A][C_{12}]}{1 + K_{A6}[C_6] + K_{A12}[C_{12}]} - V_i \cdot d_C \cdot [C_{12}] \quad (\text{S30c})$$

By dividing out the volumes from the derivatives on the left-hand sides, and assuming that V (the total volume) is constant and d_C is negligible, we obtain

$$\frac{d[A]}{dt} = a_A \cdot f_{\text{Pbad}}(\text{Ara}) - (d_A + \gamma) \cdot [A] \quad (\text{S31a})$$

$$\frac{d[C_6]}{dt} = -d_{A6} \cdot c \cdot \frac{[A][C_6]}{1 + K_{A6}[C_6] + K_{A12}[C_{12}]} - \quad (\text{S31b})$$

$$\frac{d[C_{12}]}{dt} = -d_{A12} \cdot c \cdot \frac{[A][C_{12}]}{1 + K_{A6}[C_6] + K_{A12}[C_{12}]} \quad (\text{S31c})$$

where γ is the dilution factor as before and $c = \frac{V_i}{V}$ is the cell density from above.

As AiiA concentrations are never observed, we can arbitrarily rescale $[A]$, reducing the parametric complexity of the model. By substituting $[A] = k_A \cdot a$, we obtain

$$\frac{da}{dt} = f_{\text{Pbad}}([C_6], [C_{12}]) - (d_A + \gamma)a \quad (\text{S32a})$$

$$\frac{d[C_6]}{dt} = -c \cdot \hat{d}_6 \cdot \frac{a \cdot [C_6]}{1 + K_{A6}[C_6] + K_{A12}[C_{12}]} \quad (\text{S32b})$$

$$\frac{d[C_{12}]}{dt} = -c \cdot \hat{d}_{12} \cdot \frac{a \cdot [C_{12}]}{1 + K_{A6}[C_6] + K_{A12}[C_{12}]} \quad (\text{S32c})$$

Finally, we note that the equations above can be trivially concatenated with the equations of the double receiver device described in the previous section to produce a full model of each relay device.

Characterization experiment

We measured the Degradator circuit in response to varying concentrations of the arabinose inducer.

We used (uninformative) uniform priors on the previously uncharacterized parameters, and (informative) truncated Gaussian priors on parameters that had been previously characterized with mean and standard deviation taken from the marginal posteriors of the Receivers and Inducer circuit characterizations. We also use uninformative priors on the B_k^{back} parameters, without propagating their marginal posteriors from previous circuits.

Implementation with GEC/CRN language

We define a module for the AiiAenzyme, which includes the modelled enzymatic degradation of C6 and C12. As before, we use a rate expression argument to arbitrarily assign a promoter transfer function to the production rates of each enzyme. However, since AiiA concentrations are never observed, the maximal production rate can be *divided out*, as explained above, and without loss of generality set to a value 1.

```

1 module AiiA(P,aI,growth,capacity) = {
2   ->[[capacity]*aI*[P]] aiiA |
3   aiiA ->{daiiA} |
4   aiiA ->[[growth]*[aiiA]] |
5   c6 -> [[x]*dA6*[c6]*[aiiA]] |
6   c12 -> [[x]*dA12*[c12]*[aiiA]]
7 }

```

The GEC implementation of the Degradator circuit becomes

```

1 device drR33S175() = { LuxR(aR33,growth,capacity) | LasR(aS175,growth,capacity) |
   YFP(P81,aYFP,growth,capacity) | CFP(P76,aCFP,growth,capacity) }
2 device pBadAiiA() = { AiiA(PBAD,1.0,growth,capacity) }
3
4 system aiiA = {
5   directive simulation { final=36.0; points=250; plots=[[x]*([yfp]+[f530])+b530;
   [x]*([cfp]+[f480])+b480]; plotcolours=["#FFDF00"; "#ADD8E6"] }
6   directive parameters [
7     r = 1, { interval=Real; distribution=Uniform(0.1,10); variation=Multiple };
8     K = 2, { interval=Real; distribution=Uniform(0.1,5); variation=Multiple };
9     tlag = 1, { interval=Real; distribution=Uniform(0,10); variation=Multiple };
10    rc=1e2, { interval=Log; distribution=Uniform(1e0,1e5); variation=Multiple };
11    b530=1e3, { interval=Real; distribution=Uniform(0.0,5e3); variation=Random };
12    b480=1e3, { interval=Real; distribution=Uniform(0.0,1e4); variation=Random };
13  ]
14  directive rates [growth = [grow]*r*(1 - [x] / K);capacity = rc]
15  directive deterministic {reltolerance=1e-12; abstolerance=1e-10}
16  directive crn { cells(growth,tlag) | autofluorescence(growth,capacity) }
17  | drR33S175:device
18  | pBADAiiA:device
19 }

```

Characterization results

We show results for direct and ratiometric dynamic characterization for the AiiA circuit under the TargetSwitch hypothesis.

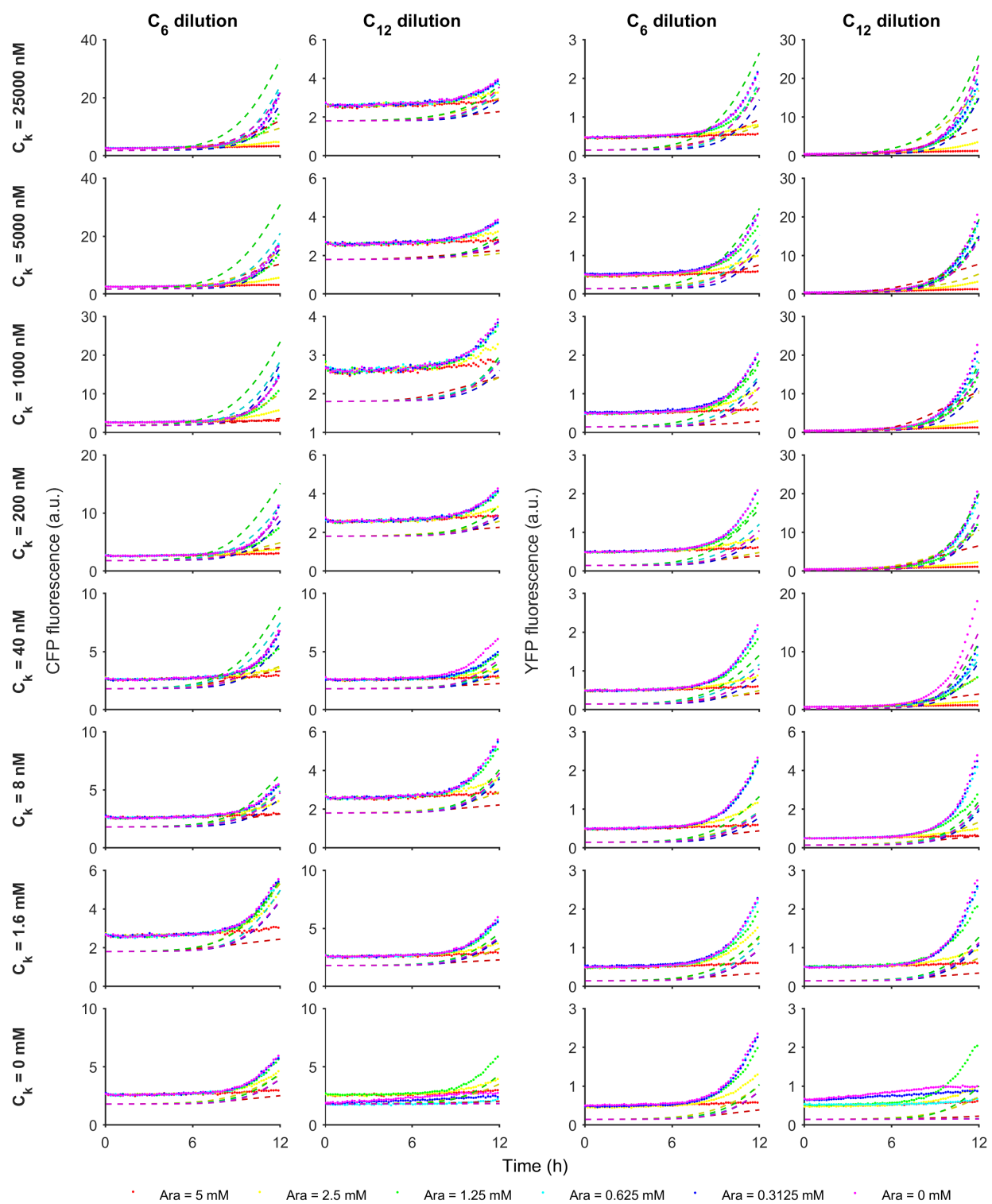


Figure S21: Model-data comparison for the Degradar circuit with the TargetSwitch hypothesis: direct method. Measurements of the TargetSwitch circuit are compared against simulations of the maximum likelihood parameter set from the TargetSwitch hypothesis.

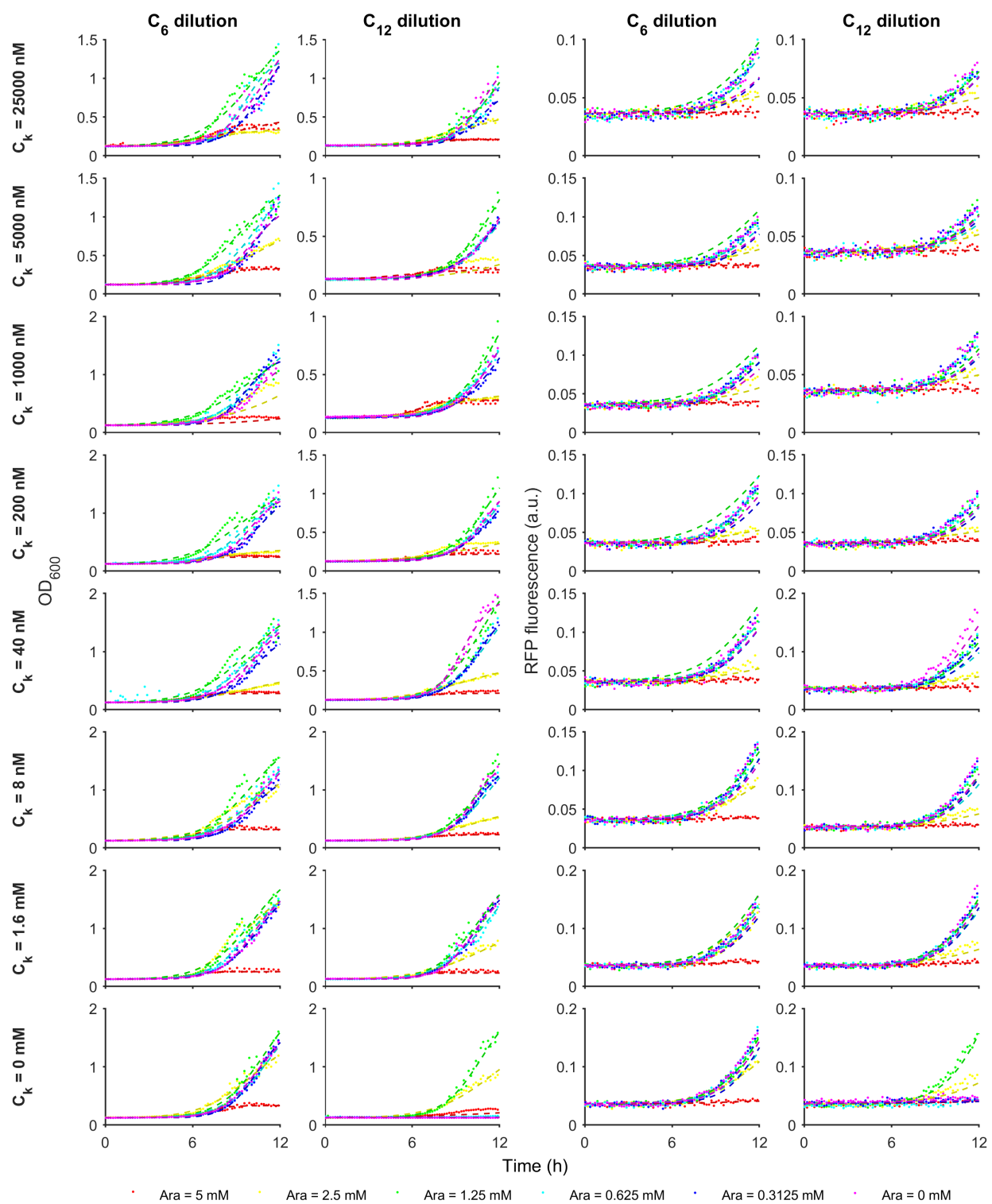


Figure S22: Model-data comparison for the Degradar circuit with the TargetSwitch hypothesis: OD and control phase. Measurements of the Degradar circuit are compared against simulations of the maximum likelihood parameter set from the TargetSwitch hypothesis.

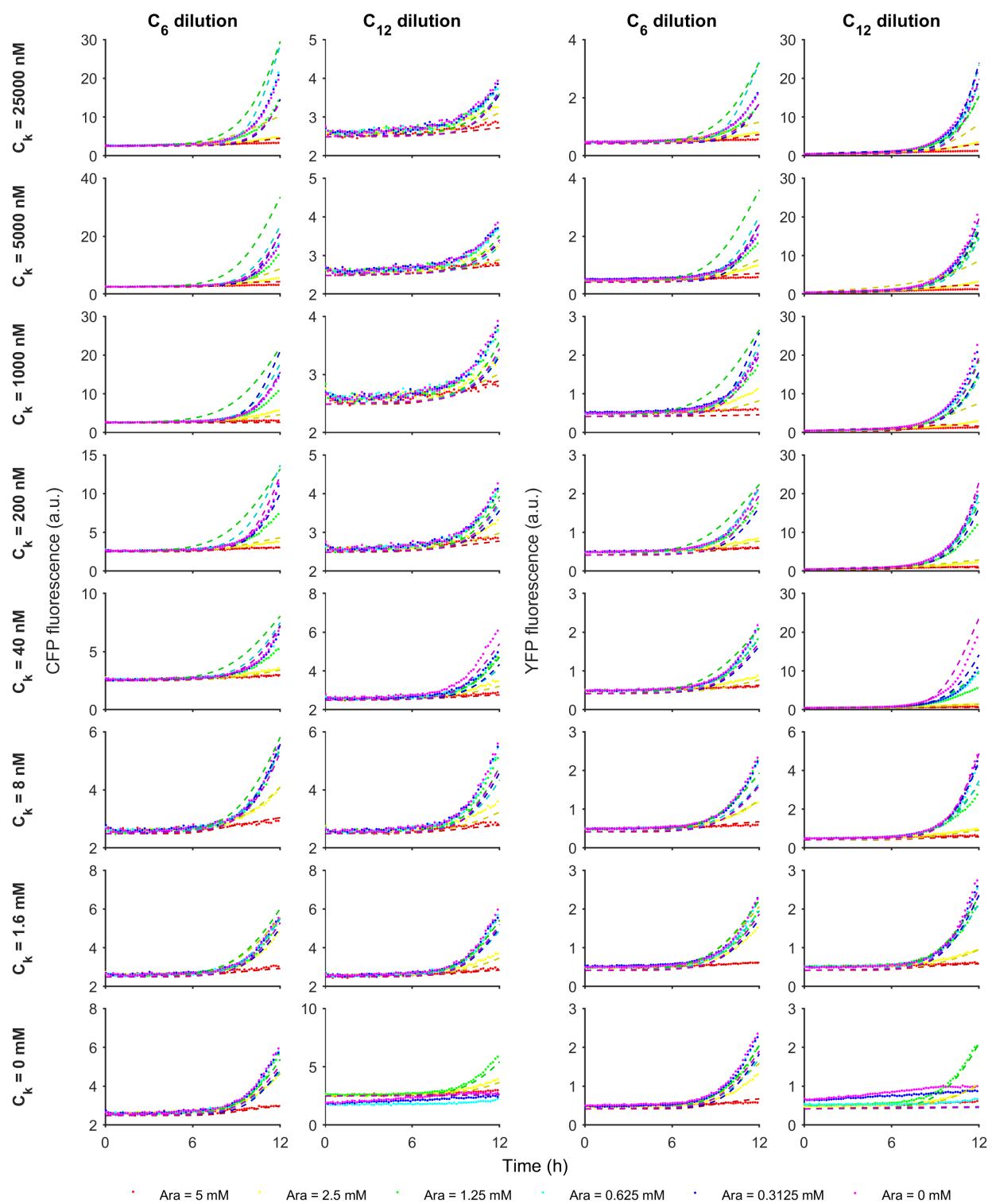


Figure S23: Model-data comparison for the Degradar circuit with the TargetSwitch hypothesis: ratiometric method. Measurements of the Degradar circuit are compared against simulations of the maximum likelihood parameter set from the TargetSwitch hypothesis.

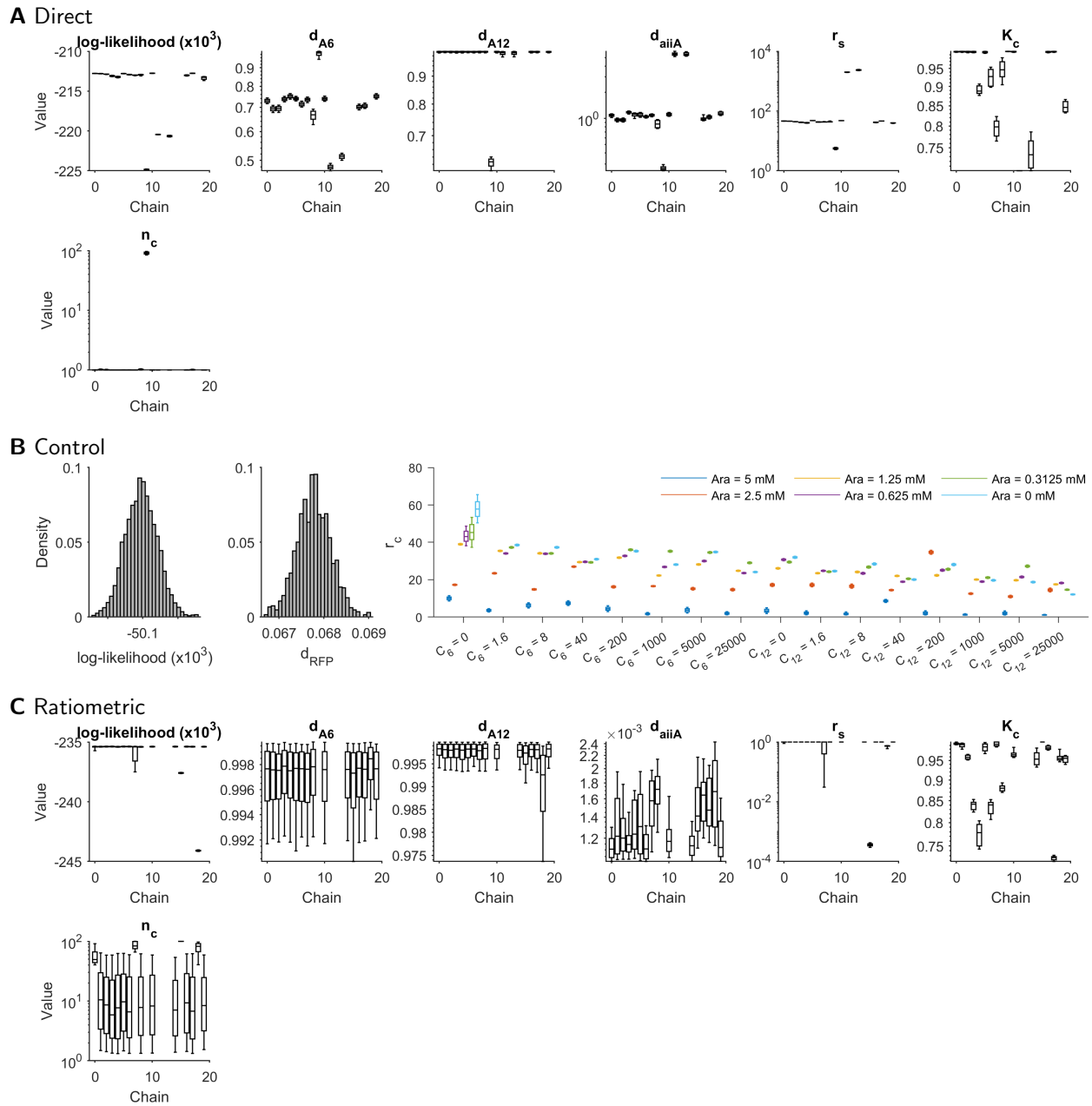


Figure S24: Marginal parameter posterior distributions for the Degradar circuit with TargetSwitch hypothesis. A. Inference of circuit parameters using the direct (non-ratiometric) method, which corresponds to assuming that $r_c = 1$ for all time-series traces. **B.** The control phase identifies values for r_c for each time-series, to be used in ratiometric characterization. **C.** Inference of circuit parameters using the ratiometric method, using the values of r_c in B.

S3 Supplementary Figures and Tables

Table S1: Plasmids not previously described.

Plasmid name	Promoter	RBS	CDS	Origin/antibiotic
PRPR	PR	B0034	eCFP; eYFP	P15/aKan
PBAD-YFP	PBAD	B0034	eYFP	PSC101/Chlor
PBAD-AiiA	PBAD	B0034	AiiA	PSC101/Chlor

Table S2: Parts Database

Part Name	Part Type	BioBrick Id
pLas81	Promoter	-
pLux76	Promoter	-
pBAD	Promoter	BBa_I0500
pCat	Promoter	BBa_I4033
pLac	Promoter	BBa_R0011
pTet	Promoter	BBa_R0040
pr	Promoter	BBa_R0051
rbs900	RBS	-
rbsS100	RBS	-
rbsS175	RBS	-
rbs32	RBS	BBa_B0032
rbs33	RBS	BBa_B0033
rbs34	RBS	BBa_B0034
mrfp1	PCR	-
aiaa	PCR	BBa_C0060
luxI	PCR	BBa_C0161
lasI	PCR	BBa_C0178
ecfp	PCR	BBa_E0420
eyfp	PCR	BBa_E0430
luxR	PCR	BBa_J69010
lasR	PCR	BBa_J69121
l3s2p21	Terminator	-
ter1	Terminator	BBa_B0015

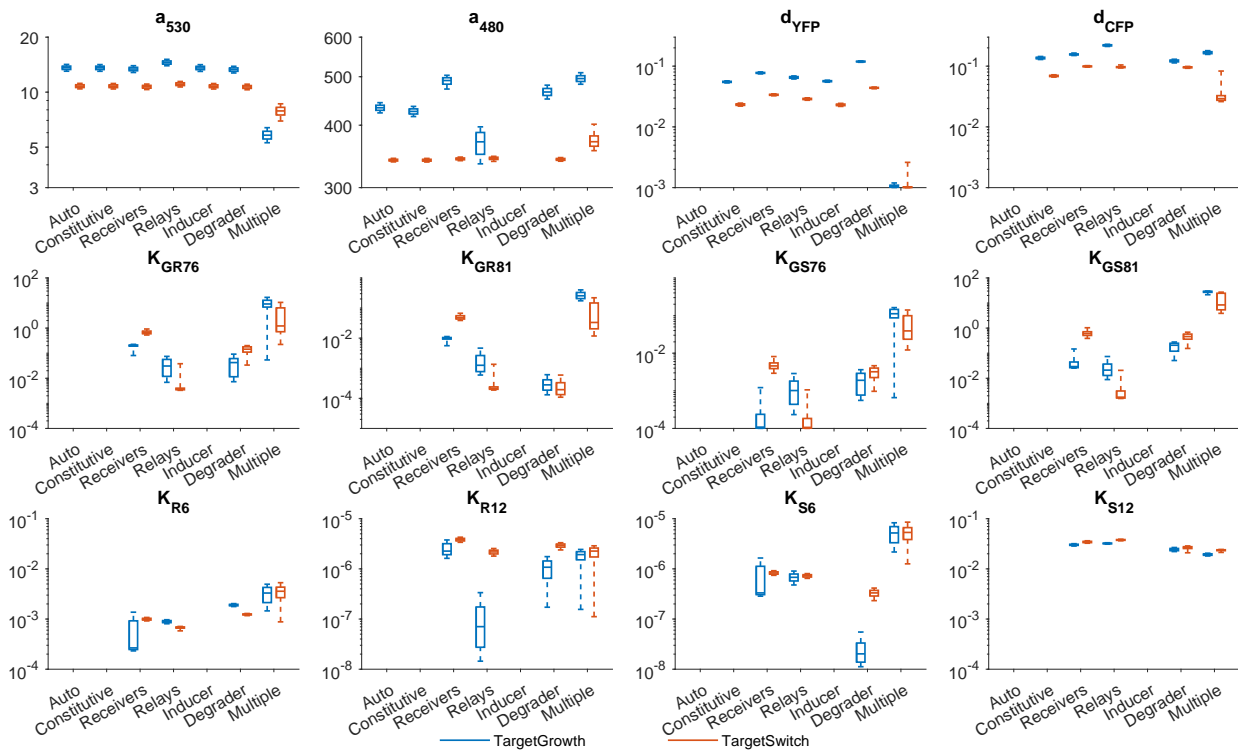


Figure S25: Evolution of marginal parameter distributions using direct dynamic characterization.

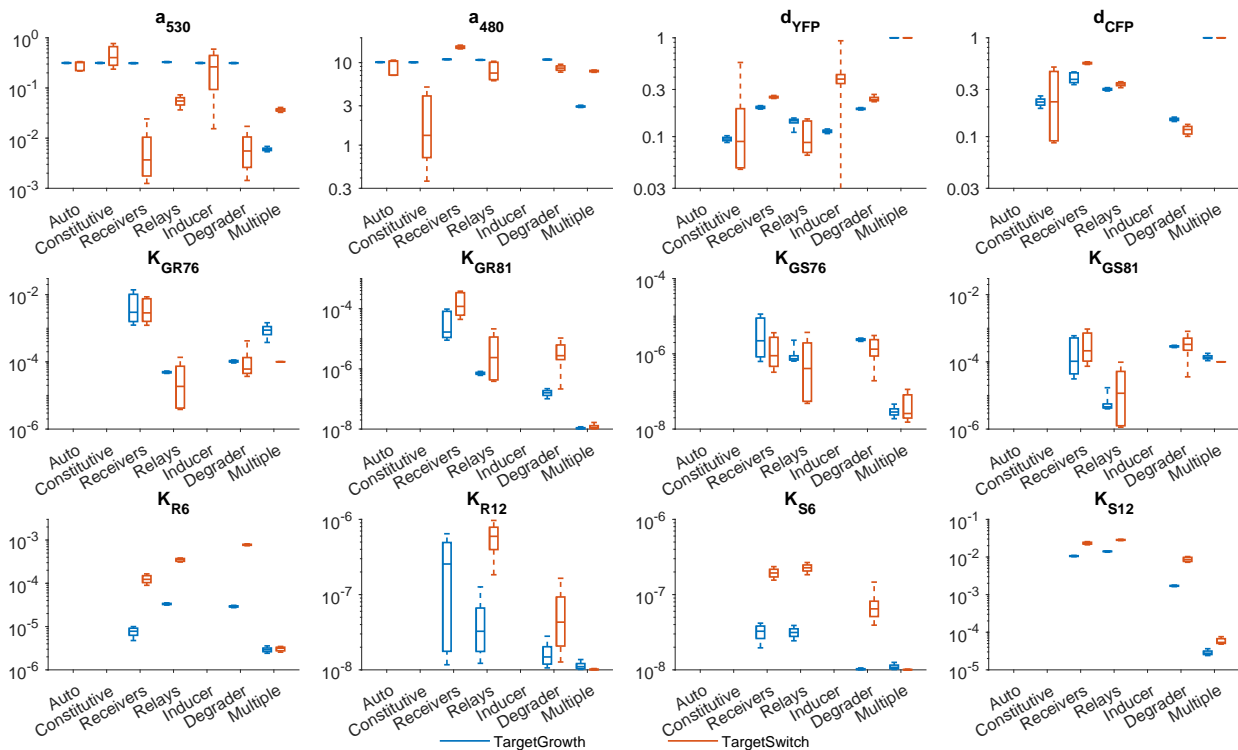


Figure S26: Evolution of marginal parameter distributions using ratiometric dynamic characterization.

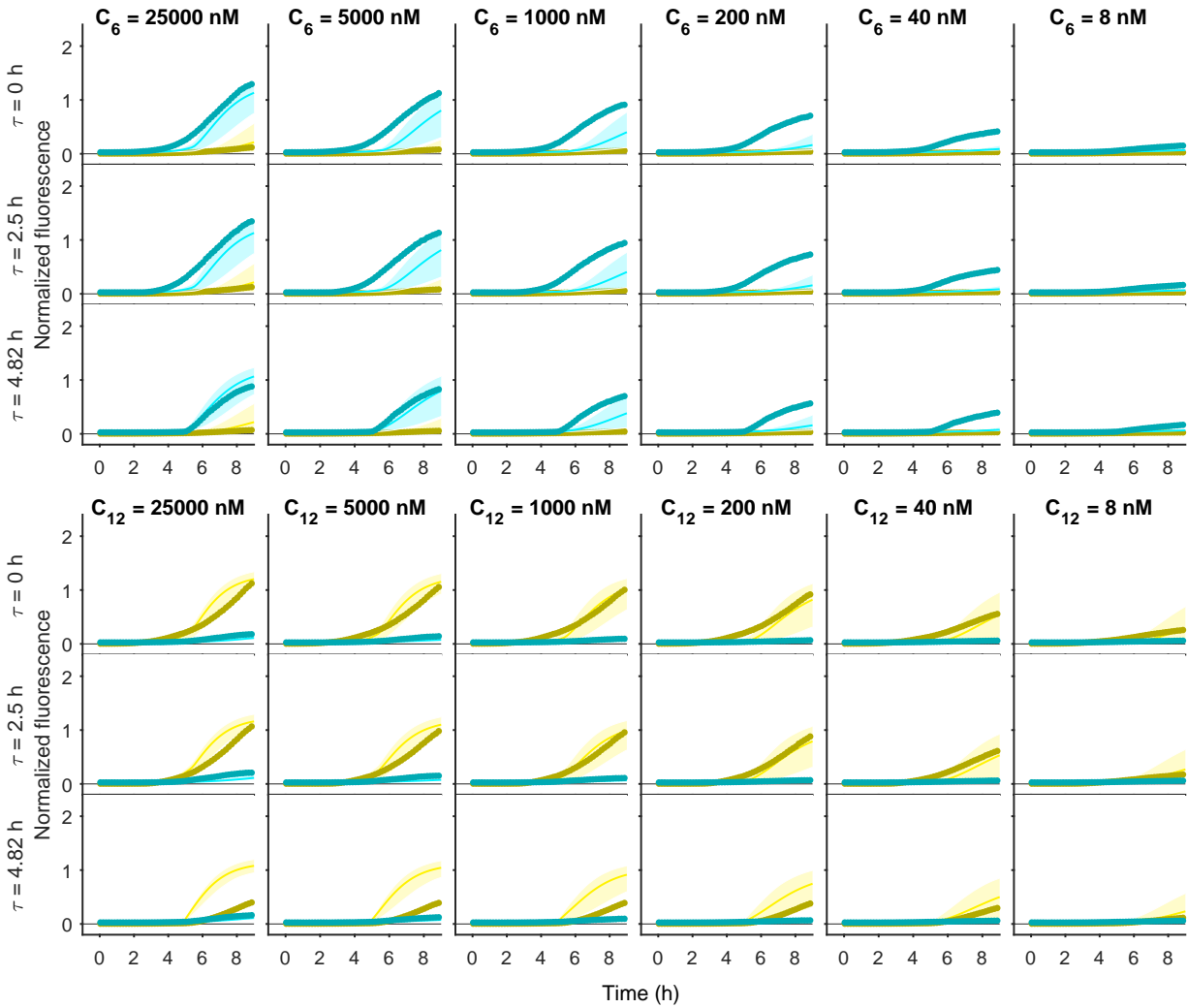


Figure S27: Prediction of unseen data. Comparison of the posterior predictive distribution for the TargetSwitch model using the ratiometric simultaneous method. In each column, the HSL treatment is indicated at the top, and in each row the time of HSL addition is noted on the left. eYFP and eCFP data are shown as thick darker lines (yellow and cyan respectively), with model simulations depicted as the mean (thin solid lines) and 95% credibility intervals as the shaded region.

Table S3: Device Database

Device Name	Components
auto	pr; rbs34; mrfp1; ter1
prpr	pr; rbs34; eyfp; ter1; pr; rbs34; ecfp; ter1
drPCat	pCat; rbs34; luxR; rbs34; lasR; ter1; pLas81; rbs34; eyfp; ter1; plx76; rbs34; ecfp; ter1
drR100S32	pTet; rbs100; luxR; ter1; pLac; rbs32; lasR; ter1; pLas81; rbs34; eyfp; ter1; plx76; rbs34; ecfp; ter1
drR33S32	pTet; rbs33; luxR; ter1; pLac; rbs32; lasR; ter1; pLas81; rbs34; eyfp; ter1; plx76; rbs34; ecfp; ter1
drR33S175	pTet; rbs33; luxR; ter1; pLac; rbsS175; lasR; ter1; pLas81; rbs34; eyfp; ter1; plx76; rbs34; ecfp; ter1
relayP76LasI	pLux76; rbs900; lasI; l3s2p21
relayP81LuxI	pLas81; rbs32; luxI; l3s2p21
pBADYFP	pBAD; rbs34; eyfp; l3s2p21
pBADAiiA	pBAD; rbs34; aiiA; l3s2p21

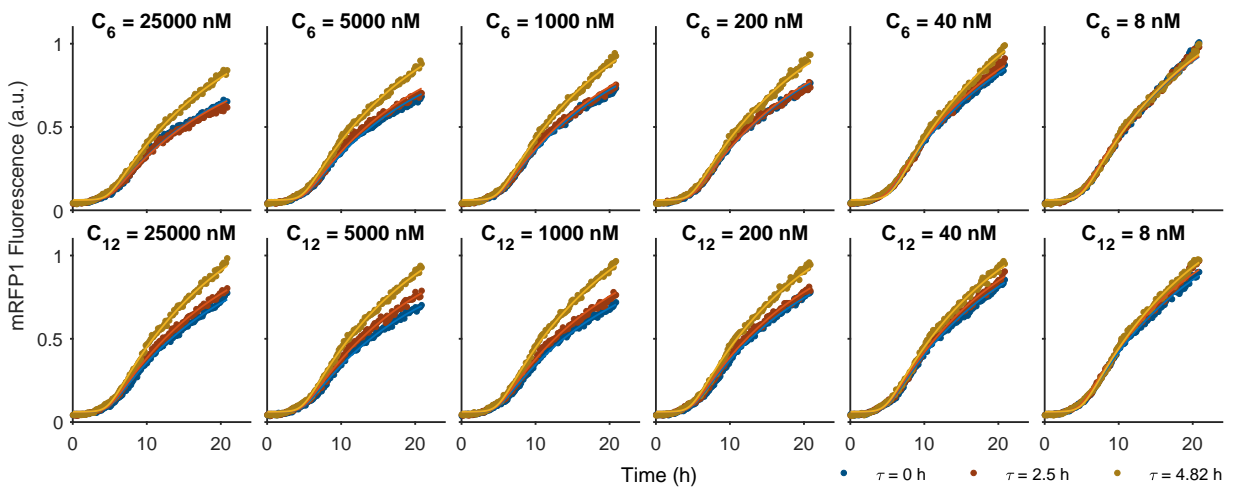


Figure S28: RFP expression in R33-S175 following delayed HSL treatment.

References

- [1] C. Spaccasassi, N. Dalchau, M. Lakin, R. Petersen, and A. Phillips, "Visual DSD User Manual." https://www.microsoft.com/en-us/research/uploads/prod/2009/02/Visual_DSD_Manual.pdf.
- [2] M. Pedersen and A. Phillips, "Towards programming languages for genetic engineering of living cells," *Journal of the Royal Society Interface*, vol. 6, no. suppl.4, pp. S437–S450, 2009.
- [3] P. K. Grant, N. Dalchau, J. R. Brown, F. Federici, T. J. Rudge, B. Yordanov, O. Patange, A. Phillips, and J. Haseloff, "Orthogonal intercellular signaling for programmed spatial behavior," *Molecular systems biology*, vol. 12, no. 1, p. 849, 2016.
- [4] C. Smith, H. Song, and L. You, "Signal Discrimination by Differential Regulation of Protein Stability in Quorum Sensing," *Journal of Molecular Biology*, vol. 382, no. 5, pp. 1290–1297, 2008.
- [5] T. Danino, O. Mondragón-Palomino, L. Tsimring, and J. Hasty, "A synchronized quorum of genetic clocks," *Nature*, vol. 463, pp. 326–330, jan 2010.
- [6] Y. Chen, J. K. Kim, A. J. Hirning, K. Josi, and M. R. Bennett, "Emergent genetic oscillations in a synthetic microbial consortium," *Science*, vol. 349, pp. 986–989, aug 2015.
- [7] D. Liu, J. Momb, P. W. Thomas, A. Moulin, G. A. Petsko, W. Fast, and D. Ringe, "Mechanism of the quorum-quenching lactonase (AiiA) from *Bacillus thuringiensis*. 1. Product-bound structures," *Biochemistry*, vol. 47, no. 29, pp. 7706–7714, 2008.